Supporting Information

for

Bipyridine based metallogels: An unprecedented difference in photochemical and chemical reduction in the *in situ* nanoparticle formation

R. Tatikonda,[a] K. Bertula,[b] Nonappa,[b] S. Hietala,[c] K. Rissanen[a*] and M. Haukka[a*]

[a]Department of Chemistry, Nanoscience Center, University of Jyväskylä, P.O. Box 35, 40014 Jyväskylä, Finland.

[b] Department of Applied Physics, Aalto University School of Science, Puumiehenkuja 2, FI-02150, Espoo, Finland.

[c] Department of Chemistry, Laboratory of Polymer Chemistry, University of Helsinki, P.O.Box 55, FI-00014, Finland.

Table of Contents

1. Experimental section

1.1 General and analytical procedures

All chemicals were purchased from chemical sources and used without purification. DMSO for the gelation test was ACS reagent grade (≥99.9%). 4,4´-dihydroxy-2,2´-bipyridine was synthesized by demethylation of 4,4´-dimethoxy-2,2´-bipyridine under acidic conditions. The NMR spectra (1D and 2D) of ligands and its silver Ag(I) complexes were recorded on a Bruker Avance DRX 400 and Bruker Avance III 500 NMR spectrometers and chemical shifts were expressed in ppm (Nitromethane used as external ref for ^{1}H-^{15}N COSY). UV-Vis Spectral measurements performed on Perkin Elmer Lambda 650.

1.2 General procedure for the synthesis of ligands 2, 3 and 4

A mixture of 4,4´-dihydroxy-2,2´-bipyridine (188.2 mg, 1 mmol), potassium carbonate, K_2CO_3 (276.5 mg, 2 mmol) in 30 mL of acetonitrile was stirred at room temperature for 2 h. 2- or 3- or 4-(Chloromethyl) pyridine hydrochloride (328.1 mg, 2 mmol) was added to the above mixture and heated to reflux for 36h. After the reaction time, the filtrate was collected by filtration and evaporated to dryness. The product was recrystallized from MeOH and dried under vacuum.

4,4'-bis(pyridin-2-ylmethoxy)-2,2'-bipyridine (2): ^{1}H NMR (400 MHz, $CDCl_3$) δ = 8.63 (dq, 1H), 8.51 (d, 1H), 8.50 (d, 1H), 8.10 (d, 1H), 7.73 (td, 1H), 7.52 (dt, 1H), 7.25 (m, 1H), 6.93 (dd, 1H), 5.35 (s, 2H). **^{13}C NMR (100 MHz, $CDCl_3$) δ** = 165.77, 157.98, 156.23, 150.64, 149.66, 137.15, 123.16, 121.64, 111.21, 107.96, 70.71.

^{1}H NMR (500 MHz, DMSO-d_6 at 70°C) δ = 8.59 (dq, 1H), 8.50 (d, 1H), 8.01 (d, 1H), 7.84 (dt, 1H), 7.55 (d, 1H), 7.35 (qd, 1H), 7.11 (dd, 1H), 5.36 (s, 2H). **^{1}H-^{15}N COSY NMR (DMSO-d_6 at 70°C) δ**= −68.12 (pyridine) and −94.41 (bipy).

4,4'-bis(pyridin-3-ylmethoxy)-2,2'-bipyridine (3): ^{1}H NMR (400 MHz, $CDCl_3$) δ = 8.71 (d, 1H), 8.61 (dd, 1H), 8.50 (d, 1H), 8.10 (d, 1H), 7.79 (dt, 1H), 7.34 (dd, 1H), 6.91 (dd, 1H), 5.24 (s, 2H). **^{13}C NMR (100 MHz, $CDCl_3$) δ** = 165.66, 157.99, 150.54, 150.00, 149.25, 135.56, 131.61, 123.79, 111.81, 107.01, 67.62.

^{1}H NMR (500 MHz, DMSO-d_6) δ = 8.73 (d, 1H), 8.58 (dd, 1H), 8.52 (d, 1H), 8.05 (d, 1H), 7.92 (dt, 1H), 7.45 (qd, 1H), 7.14 (dd, 1H), 5.35 (s, 2H). **^{13}C NMR (100 MHz, DMSO-d_6) δ** = 165.15, 150.62, 149.41, 149.17, 135.84, 131.79, 123.67, 111.42, 106.74, 67.07. ^{1}H-^{15}N COSY NMR (DMSO-d_6 at 30°C) δ= −64.87 (pyridine) and −95.07 (bipy).

4,4'-bis(pyridin-4-ylmethoxy)-2,2'-bipyridine (4): ^{1}H NMR (400 MHz, $CDCl_3$) δ = 8.65 (dd, 2H), 8.51 (d, 1H), 8.08 (d, 1H), 7.38 (d, 2H), 6.93 (dd, 1H), 5.26 (s, 2H). ^{13}C NMR (100 MHz, $CDCl_3$) δ 165.61, 157.79, 150.52, 150.34, 145.09, 121.69, 111.83, 107.25, 68.20.

^{1}H NMR (500 MHz, DMSO-d_6 at 70^{o}C) δ = 8.60 (dd, 2H), 8.51 (d, 1H), 8.02 (d, 1H), 7.47(d, 2H), 7.11 (dd, 1H), 5.37 (s, 2H). ^{1}H-^{15}N COSY NMR (DMSO-d_6 at 70^{o}C) δ= −65.35 (pyridine) and −94.18 (bipy).

1.3 ***Metal complexes***

[2•AgNO3]: ^{1}H NMR (500 MHz, DMSO-d_6) δ= 8.62 (dq, 1H), 8.54 (d, 1H), 8.05 (d, 1H), 7.88 (dt, 1H), 7.59 (d, 1H), 7.39 (qd, 1H), 7.22 (dd, 1H), 5.42 (s, 2H). **^{1}H-^{15}N COSY NMR (DMSO-d_6 at 70^{o}C) δ**= −71.01 (pyridine) and −112.41 (bipy).

[3•AgNO3]: ^{1}H NMR (500 MHz, DMSO-d_6) δ = 8.77 (d, 1H), 8.62 (dd, 1H), 8.59 (d, 1H), 8.18 (d, 1H), 7.99 (dt, 1H), 7.52 (qd, 1H), 7.34 (dd, 1H), 5.44 (s, 2H). **^{13}C NMR (100 MHz, DMSO-d_6) δ** = 166.10, 153.85, 151.92, 149.95, 149.63, 136.49, 131.66, 123.98, 112.03, 109.60, 67.67. ^{1}H-^{15}N COSY NMR (DMSO-d_6 at 30^{o}C) δ= −71.52 (pyridine) and −119.98 (bipy).

[4•AgNO3]: ^{1}H NMR (500 MHz, DMSO-d_6) δ = 8.63 (dd, 2H), 8.57 (d, 1H), 8.09 (d, 1H), 7.51 (d, 2H), 7.25 (dd, 1H), 5.44 (s, 2H). **^{1}H-^{15}N COSY NMR (DMSO-d_6 at 70^{o}C) δ** = −69.32 (pyridine) and −107.53 (bipy).

2. X-ray crystallography

Single crystal X-ray structure determination: The single crystals of ligands **2**–**4** were obtained by slow evaporation of chloroform solution. The X-ray diffraction data were collected on an Agilent Technologies Supernova diffractometer using Mo Kα or Cu Kα radiation. The *CrysAlisPro*[1] program packages were used for cell refinements and data reductions. Structures were solved by charge flipping method using *SUPERFLIP*[2] program or by direct methods using *SHELXS-2008*[3] program. Gaussian absorption correction was applied to all data and structural refinements were carried out using *SHELXL-2015*[3] software.

2.1 Crystal Packing

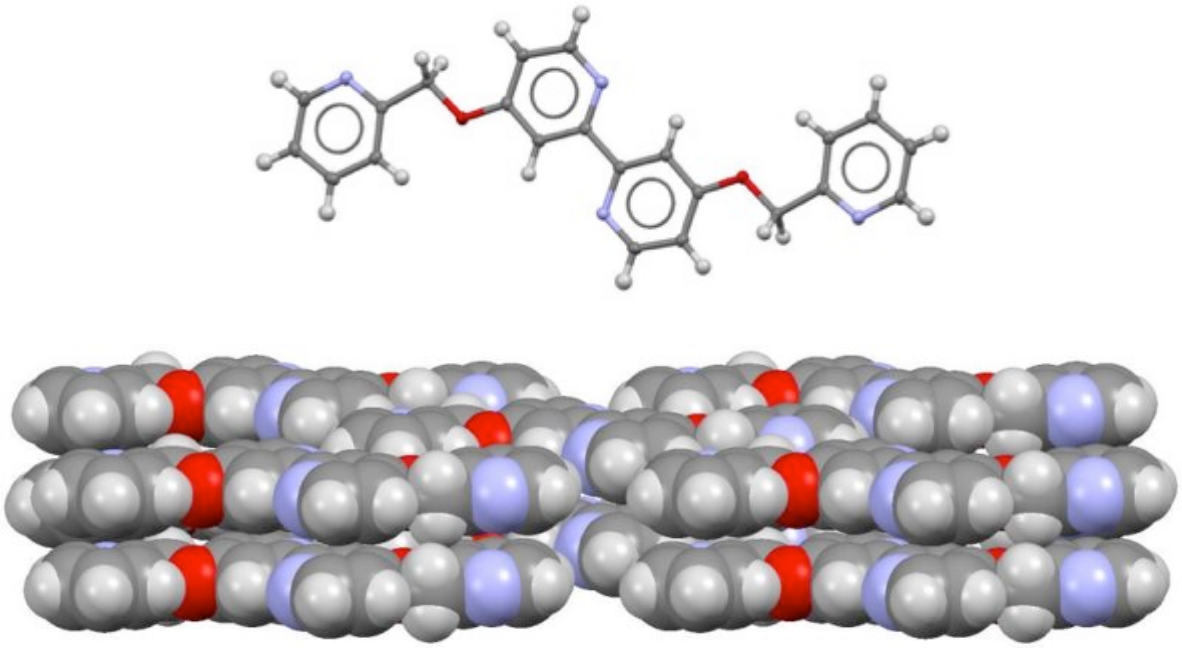

Fig. S1. Molecular structure and space filled model of crystal packing of Ligand **2.**

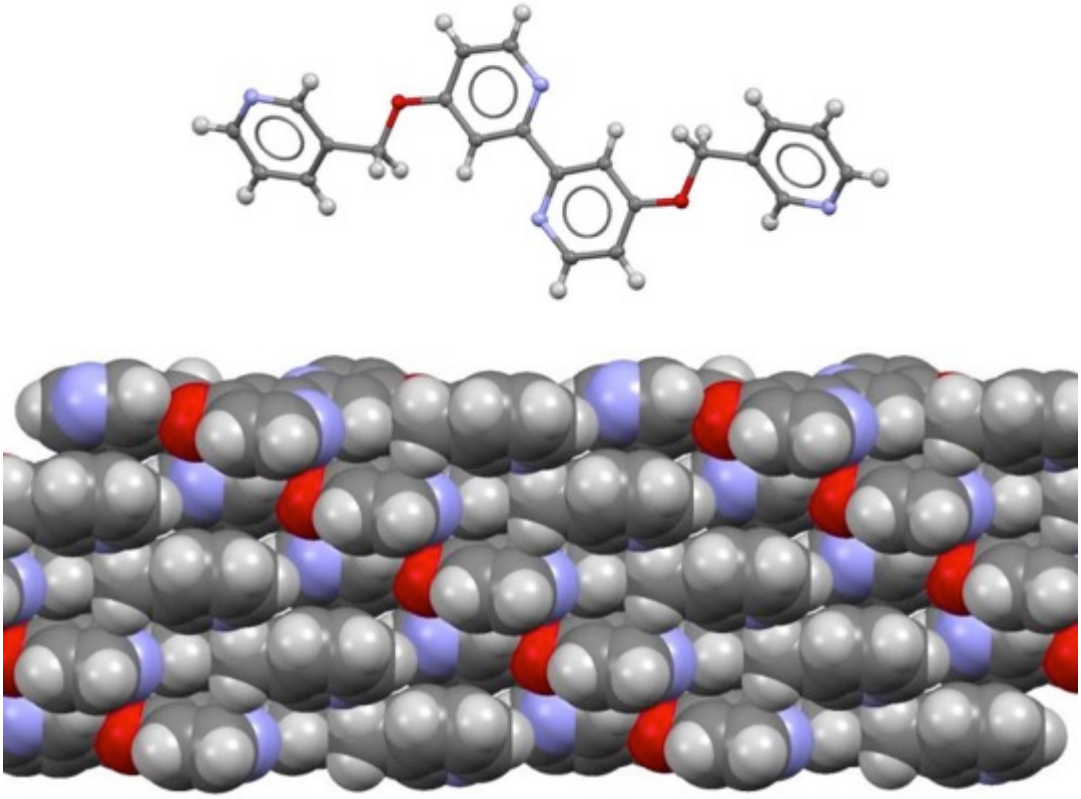

Fig. S2. Molecular structure and space filled model of crystal packing of Ligand **3.**

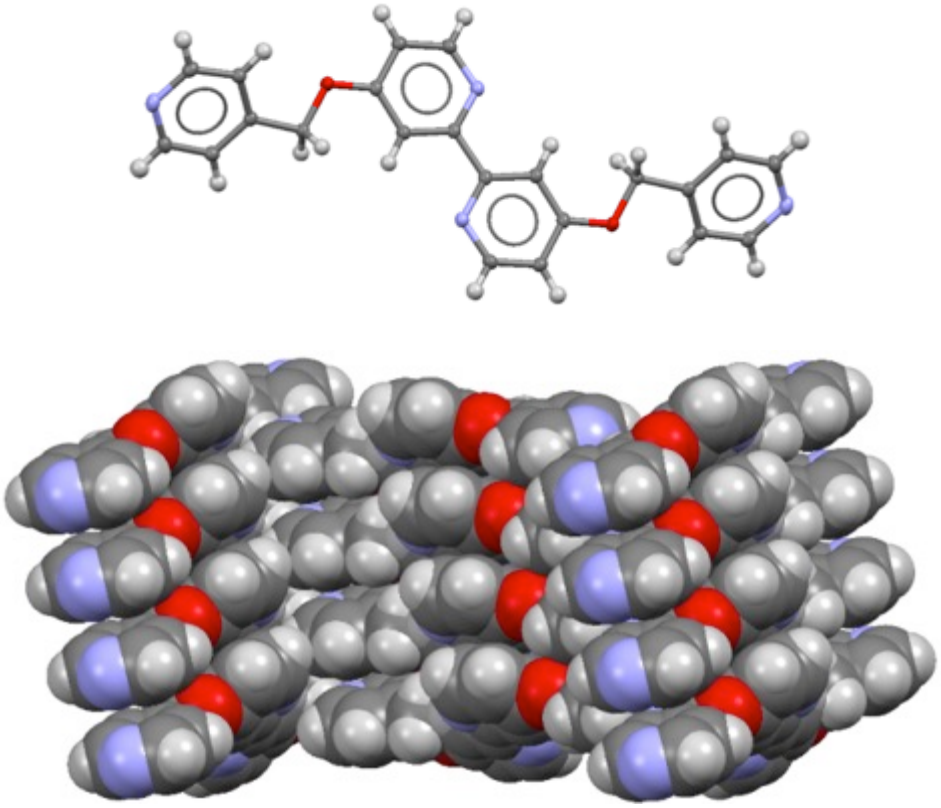

Fig. S3. Molecular structure and space filled model of crystal packing of Ligand **4.**

Table S1. Crystallographic data of ligands **2, 3** and **4**

	2	**3**	**4**
CCDC No.	1500637	1500638	1500639
Formula	$C_{22}H_{18}N_4O_2$	$C_{22}H_{18}N_4O_2$	$C_{22}H_{18}N_4O_2$
Formula weight	370.40	370.40	370.40
Temp(K)	120	120	120
Crystal System	Triclinic	Triclinic	Monoclinic
Space group	$P\ \bar{1}$	$P\ \bar{1}$	$P2_1/c$
a (Å)	3.8257(2)	6.2801(4)	3.8450(1)
b (Å)	9.9197(7)	12.0904(8)	20.0524(4)
c (Å)	11.9058(5)	13.3168(8)	11.0162(3)
α (^{o})	77.653(5)	114.646(6)	90
β (^{o})	89.013(4)	103.516(5)	90.6073(16)
γ (^{o})	80.097(6)	93.852(5)	90
V (Å^3)	434.70(5)	877.92(10)	847.69(3)
d_{calc} (g/cm^3)	1.415	1.401	1.451
Z	1	2	2
μ (mm^{-1})	0.094	0.093	0.776
Ref.Collected	5155	11863	8117
Ind. Ref	1703	3787	1781
F (000)	194	388	388
GOF	1.057	1.048	1.069
R1[a] ($I \geq 2\sigma$)	0.0353	0.0398	0.0342
wR2b($I \geq 2\sigma$)	0.0929	0.0934	0.0886

3 General procedures for gelation

Primarily the gelation experiments were performed in aqueous DMSO solvent without silver salt. Ligand **3** resulted in translucent gel at 1 wt% from 6:4 of DMSO:water solvent mixture which is gradually collapsed at room temperature during several hours of time. No gels were obtained from ligand 4 at any condition.

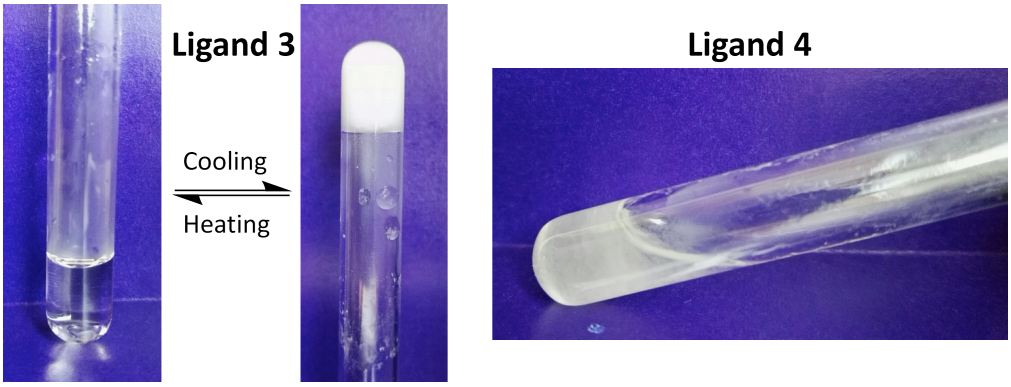

Fig. S4. Photographs showing the results from gelation tests of ligands 3 and 4 without metal complexation.

In a typical metallogelation experiment, the appropriate amounts of solid ligand (**3** or **4**) is placed in a test tube (45 x 15 mm) and dissolved in DMSO or DMF upon heating, whereupon equimolar amount of $AgNO_3$ solution in water is added to reach the final volume of 1.0 mL. The mixture is then heated to obtain a clear solution which, as it cooled down to room temperature, would afford a translucent gel. The gelation was observed at various ratios of DMSO/H_2O (v/v) and in this study four different ratios were used, viz. 8:2, 7:3, 6:4 and 1:1. Gelation was not observed when only DMSO or DMF was used as solvent. Co-solvent water is crucial for all the gelation experiments.

3.1 Chemical reduction

In chemical reduction, the gel (**3●$AgNO_3$** or **4●$AgNO_3$**) was reduced from aqueous solution of $NaBH_4$. 1.0 mL of $NaBH_4$ solution which is 20 wt % to the silver molar amount in the gel was placed on the top of the gel and allowed it for slow diffusion at room temperature. During this time, $NaBH_4$ was diffused into the gel and reduces Ag^+ to Ag^0. In **[3●$AgNO_3$]** gel, the complete reduction was observed in a week period and in **[4●$AgNO_3$]** gel the reduction was slower and takes about 3 weeks. At high wt % of $NaBH_4$ (more than 40 wt% of $NaBH_4$) the reduction was faster and gel network was collapsed.

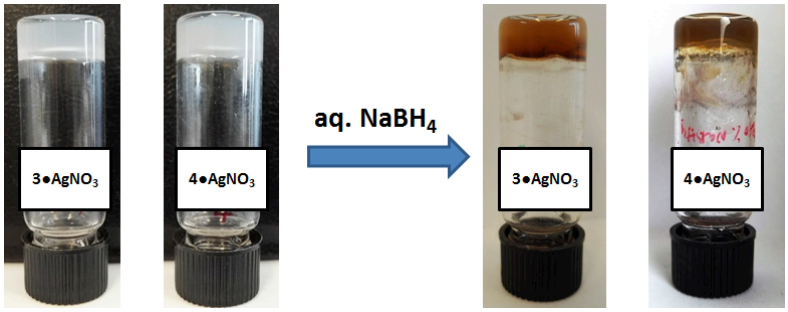

Fig. S5. Photographs showing visual color change upon chemical reduction of [**3●AgNO$_3$**] and [**4●AgNO$_3$**]

3.2 Photochemical reduction

The gels (**3**●$AgNO_3$) prepared from 8:2 and 6:4 of DMSO/H_2O was exposed to day light and photo chemical reduction was observed.

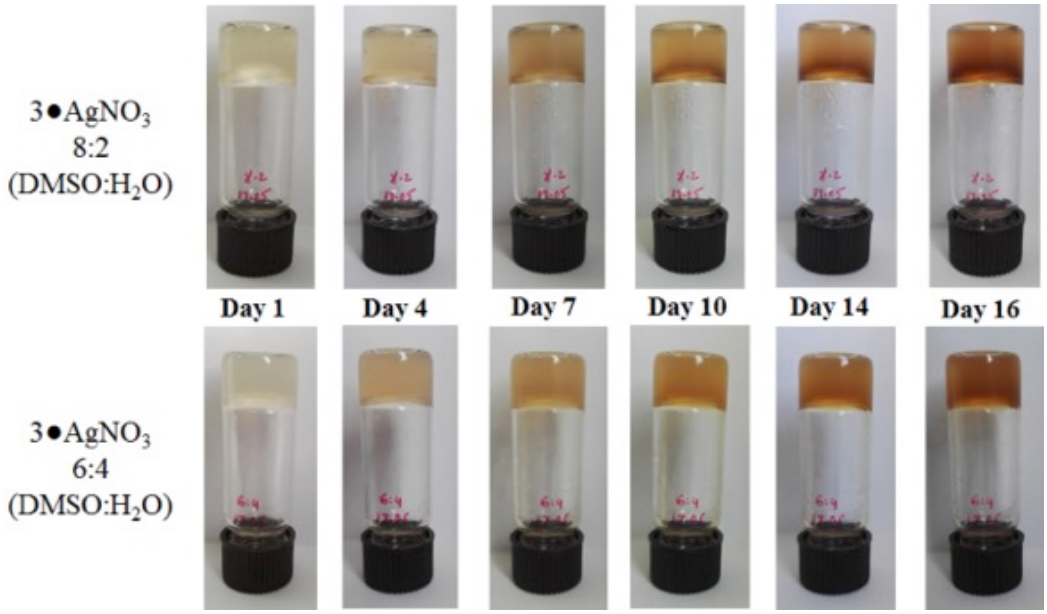

Fig. S6. Photographs showing visual color change upon daylight reduction of [**3●AgNO$_3$**].

3.3 Effect of cations on gelation of ligand 3 and 4.

Various metal salts were tested to probe the effect of metal ions on gelation. The results revealed that the gelation is cation specific, i.e. specific to silver (I). Zn, Cd and Au complexes furnished clear solutions after complexation with ligand **3**, however, upon standing overnight at room temperature, the samples precipitated. On the other hand, complexation with ligand **4** immediate precipitation was observed (Table S2).

Table S2. List of metal salts tested for gelation. (Note: ppt=precipitate)					
	$CuCl_2$	$ZnCl_2$	$CdCl_2$	$HgCl_2$	$HAuCl_4$
Ligand **3**	ppt	ppt	ppt	ppt	ppt
Ligand **4**	ppt	ppt	ppt	ppt	ppt

Table S3. List of silver salts tested for gelation. (Note: * = gels are unstable and collapsed upon standing for a few hours. Therefore, not used for rheological measurements)						
	NO_3	ClO_4	PF_6	BF_4	OTf	OAc
Ligand **3**	G	G	G	G	G	G
Ligand **4**	G	G*	G*	G*	G*	G*

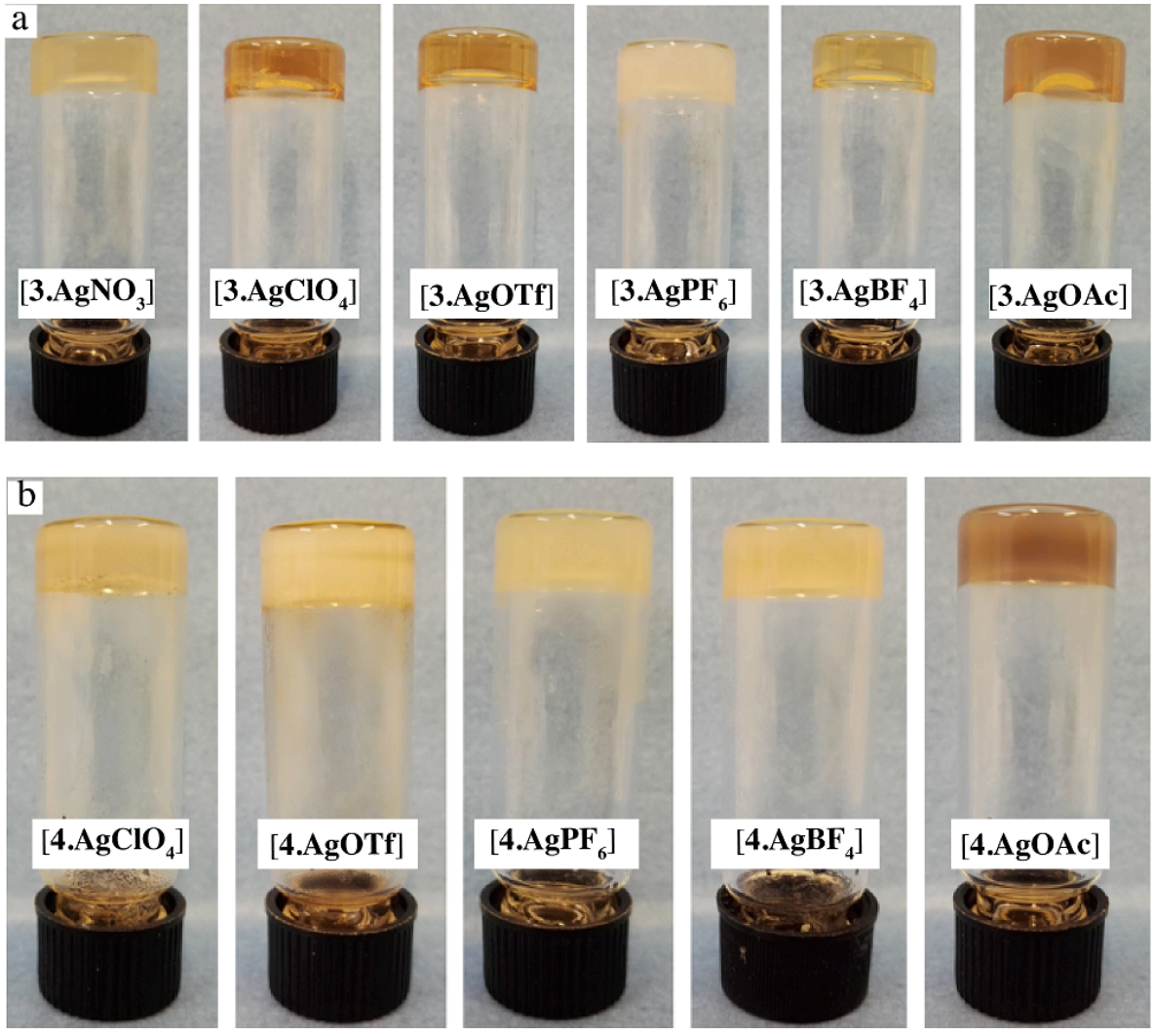

Fig. S7. Photographs of the metallogels obtained using silver salts with a) ligand **3** and b) ligand **4** in 8:2 DMSO:H_2O.

4. Scanning electron microscopy (SEM):

The sample preparation for SEM was performed by dissolving 6 mg of ligand (**3** or **4**) in 800 µL of DMSO with heating, to this clear solution equimolar amount of $AgNO_3$ in 200 µL of water was added. The resulting precipitate was solubilized by heating and let it cool down to room temperature to get a gel. The gel was then heated until it turned into a clear solution and drop casted on a carbon tape placed over aluminium stub. The sample was then allowed to dried under ambient conditions subjected for 6 nm platinum sputter coating under vacuum conditions at 20 mA for 1 min. The samples were then subjected for imaging with Sigma Zeiss scanning electron microscope.

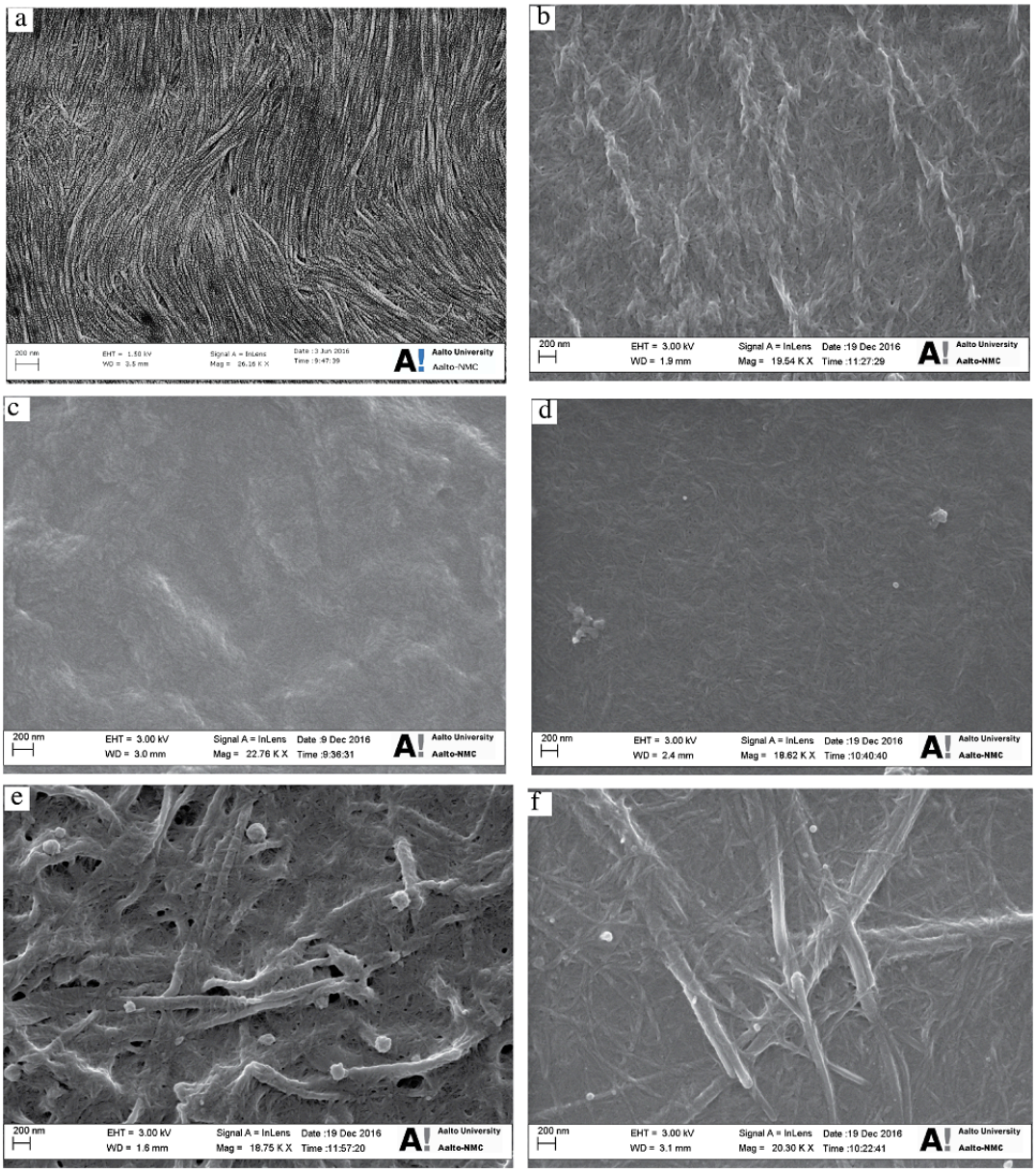

Fig. S8. SEM micrographs of xerogels derived from DMSO/H_2O gel of [**3●AgNO$_3$**]; b) [**3●AgBF$_4$**]; c) [**3●AgPF$_6$**]; d) [**3●AgClO4**]; e) [**3●AgOAc**] and f) [**3●AgOTf**].

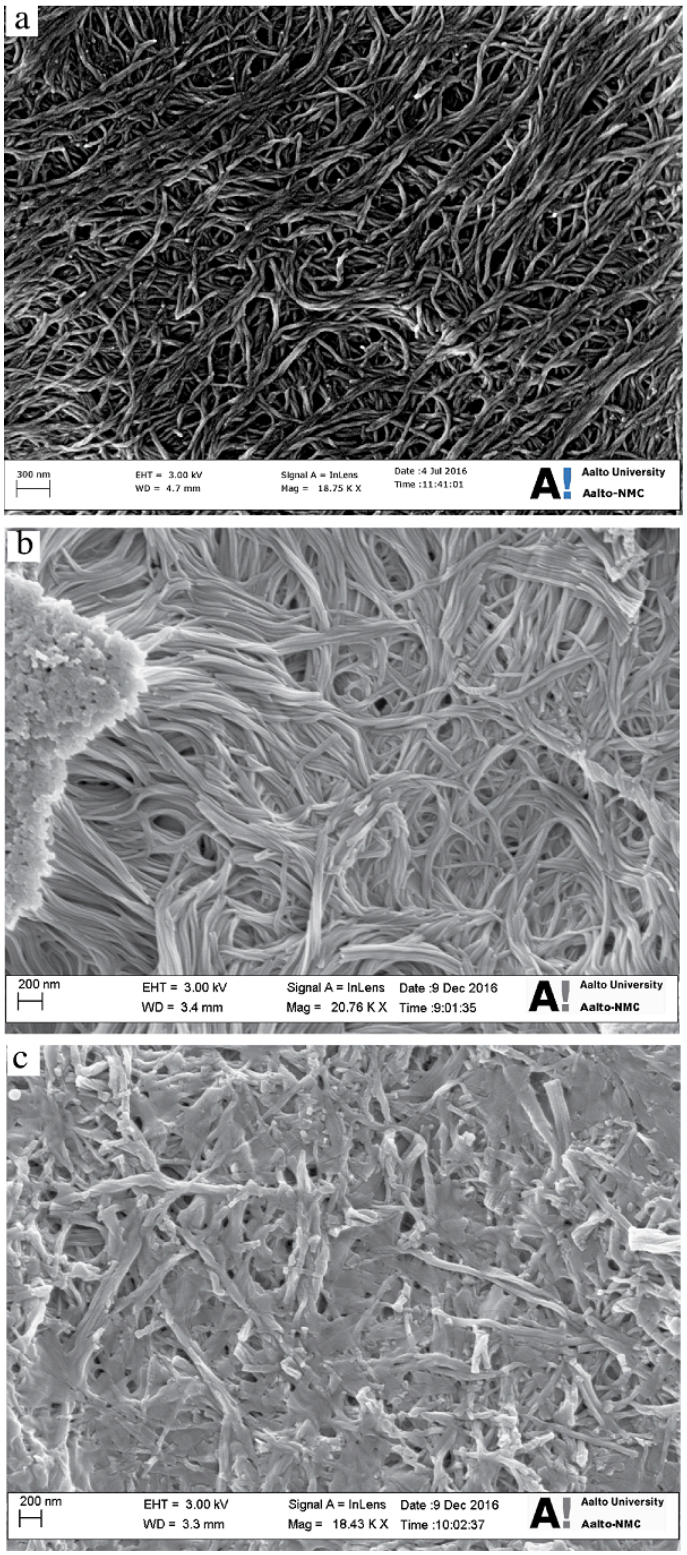

Fig. S9. SEM micrographs of xerogels derived from DMSO/H_2O gel of a) [**4●AgNO$_3$**]; b) [**4●AgBF$_4$**] and c) [**4●AgPF$_6$**].

5. Rheological measurements

TA AR2000 stress controlled rheometer equipped with 20 mm steel plate and a Peltier heated plate was used for rheological characterization. The measuring setup was covered with a sealing lid in order to prevent evaporation during the measurements. Measurements were performed using oscillation frequency of 6.284 rad/s at 20°C unless otherwise noted.

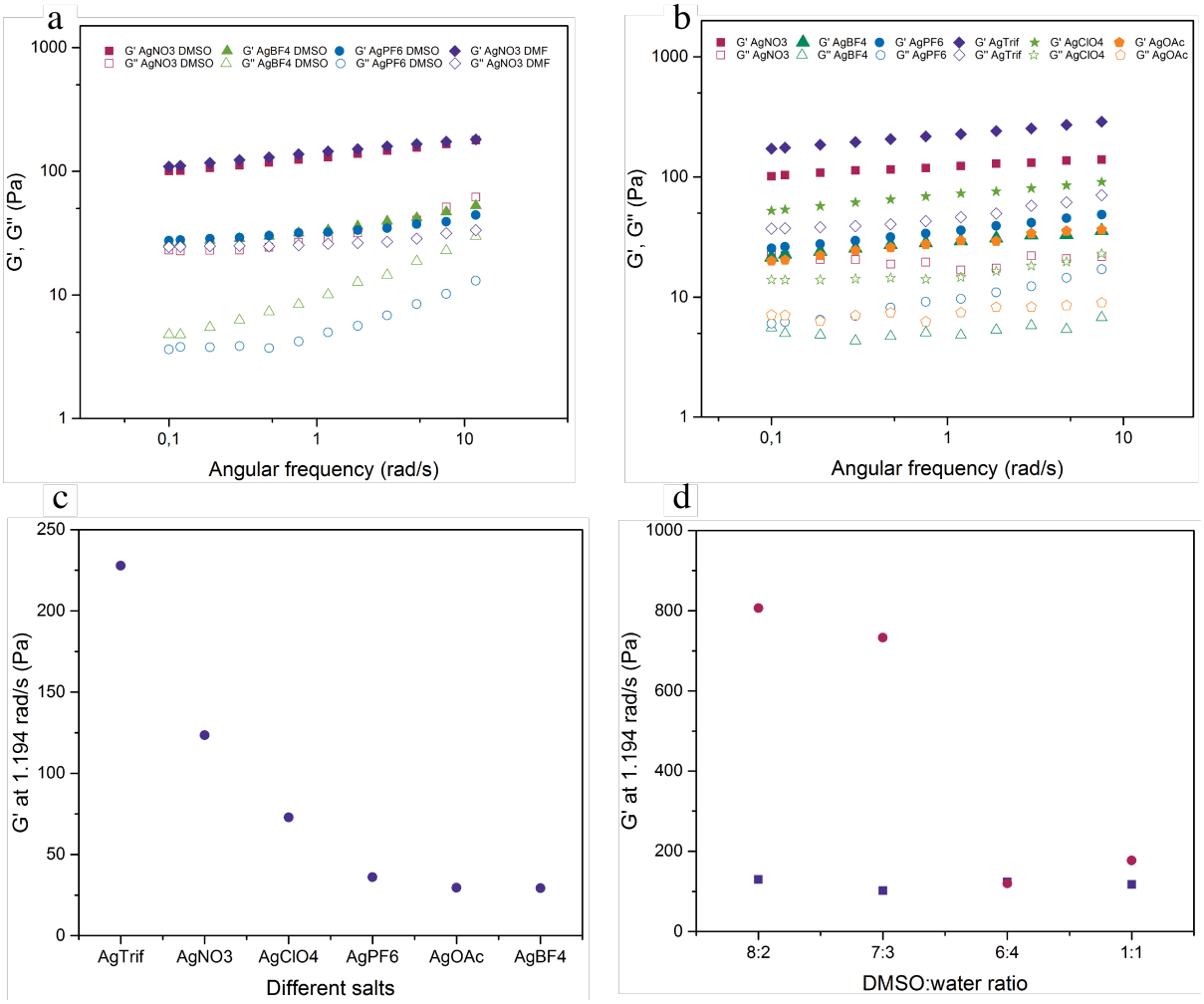

Fig. S10 Rheological properties of metallogels. a) frequency sweep experiments of as a function of different salts for gels derived from ligand **3** at 8:2 DMSO.H_2O and DMF:H_2O; b) at 6:4 DMSO:H_2O; c) shows the effect of different counter anions on the mechanical properties in DMSO:H_2O metallogels derived from ligand **3** and d) shows the effect of solvent ratio on mechanical properties of [**3●AgNO$_3$**] metallogels.

6. NMR spectroscopic studies

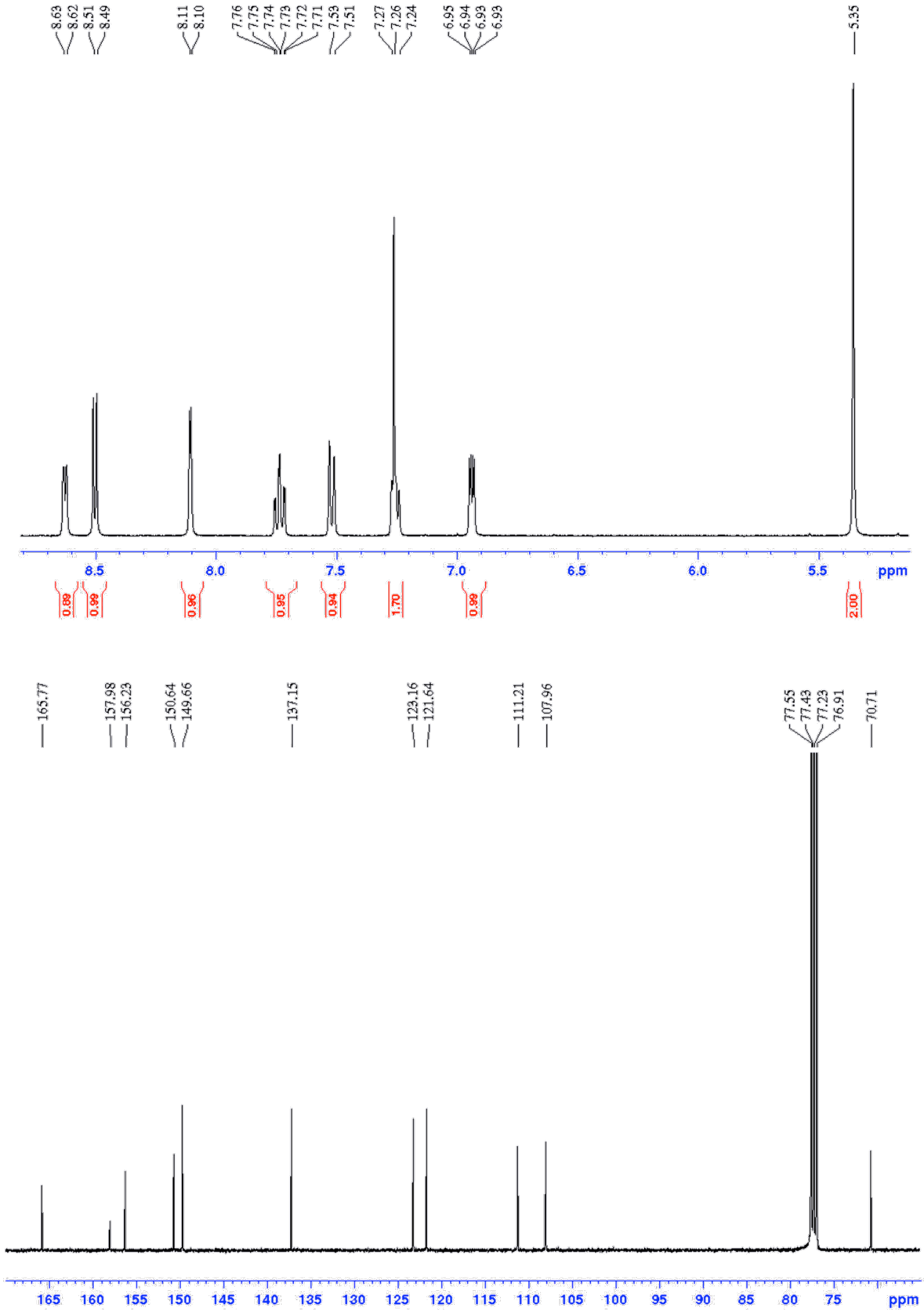

Fig. S11. ^{1}H and ^{13}C NMR of ligand **2** from $CDCl_3$.

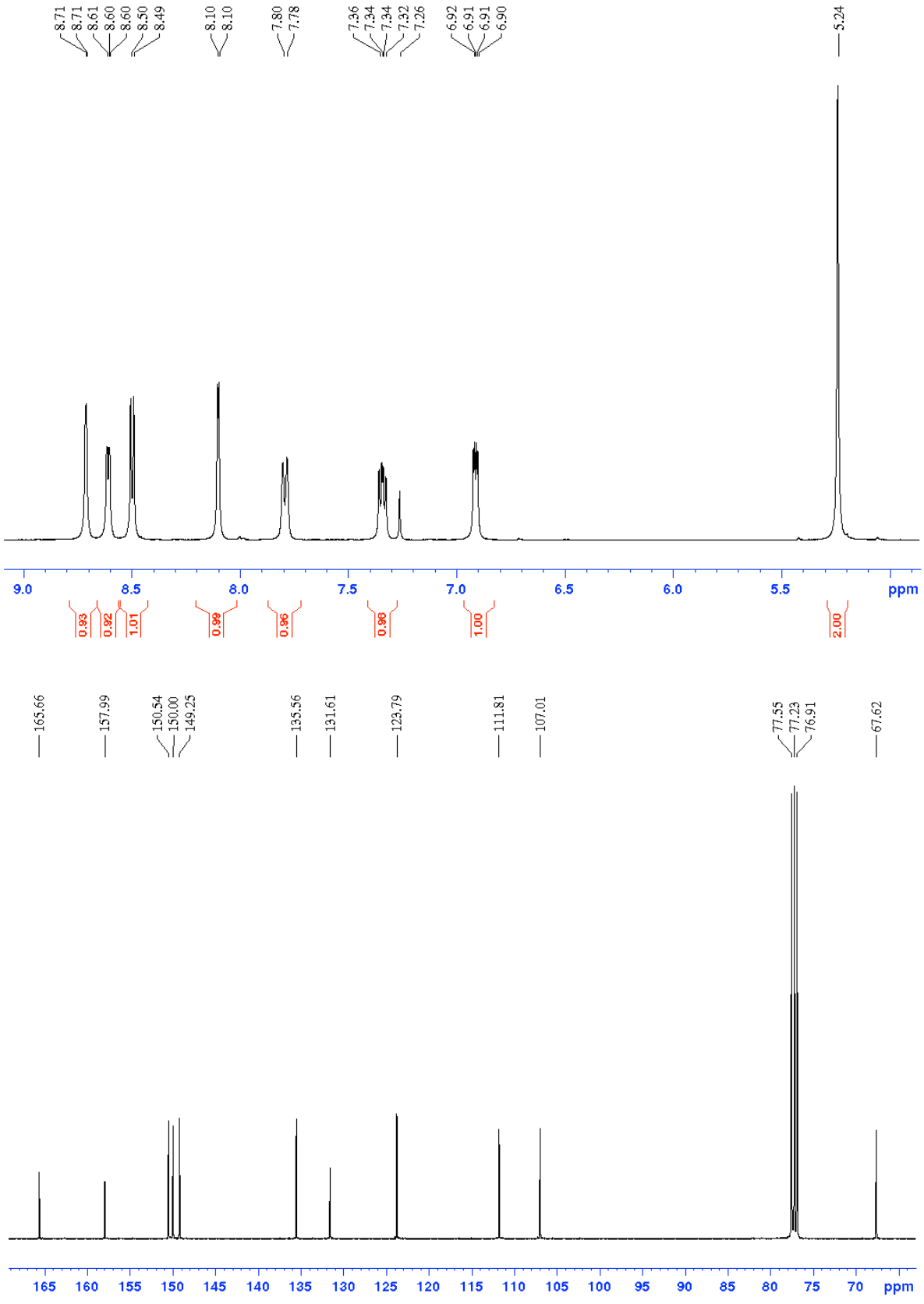

Fig. S12. ^{1}H and ^{13}C NMR of ligand **3** from $CDCl_3$.

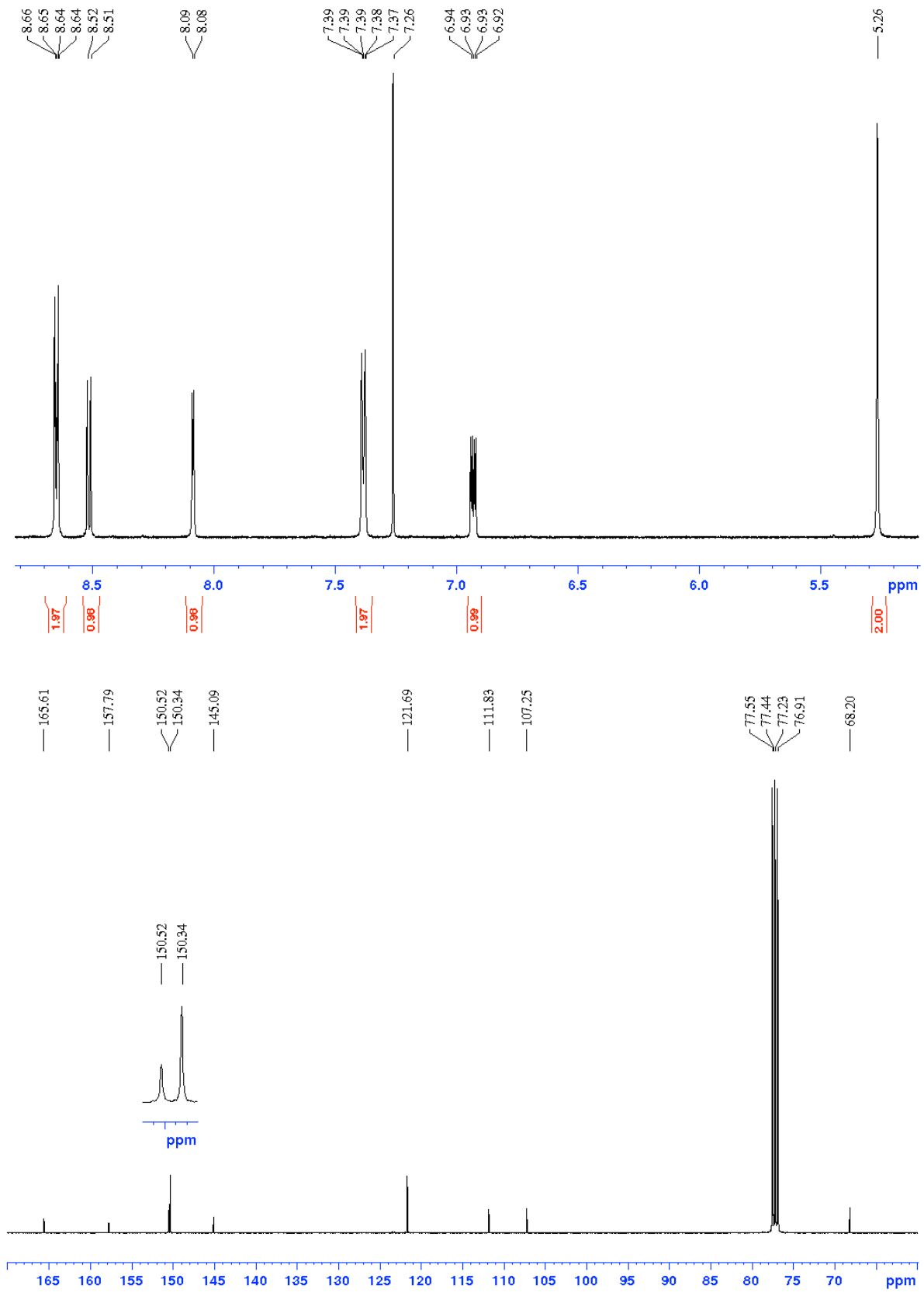

Fig. S13. ^{1}H and ^{13}C NMR of ligand **4** from $CDCl_3$.

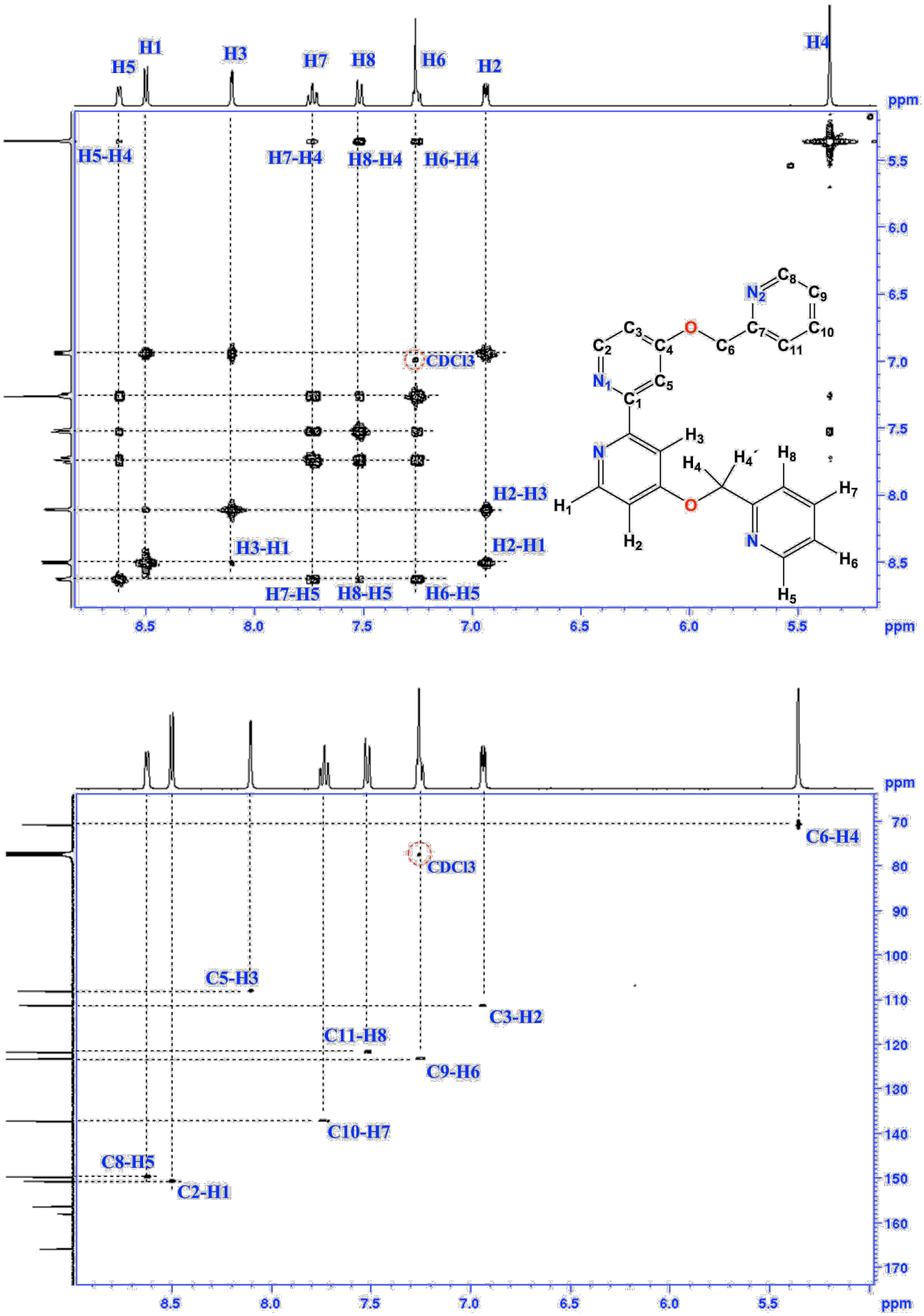

Fig. S14. 2-D NMR – COSY and HMQC for ligand **2** from $CDCl_3$.

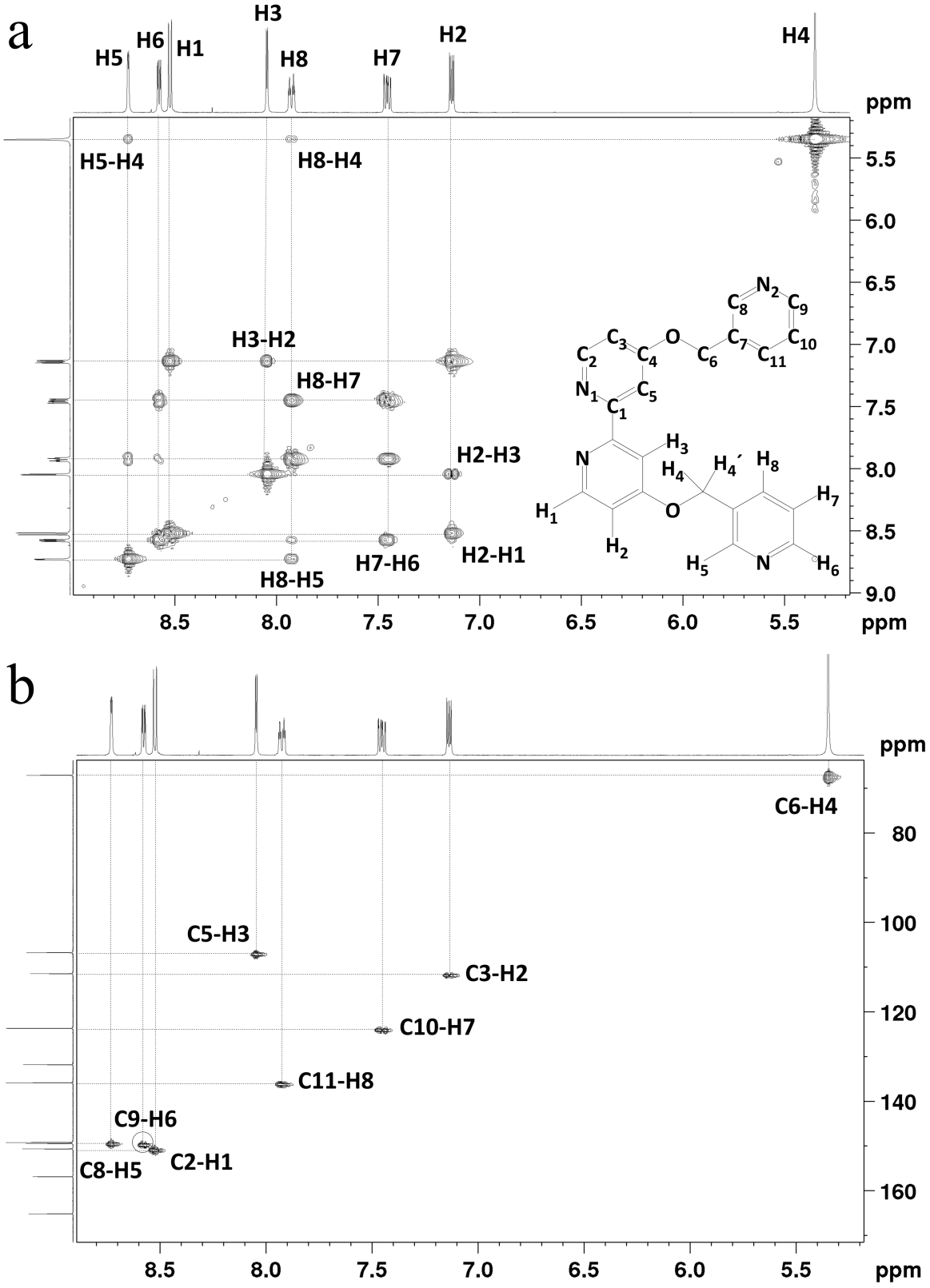

Fig. S15. 2-D NMR – COSY and HMQC for ligand **3** from DMSO-d_6.

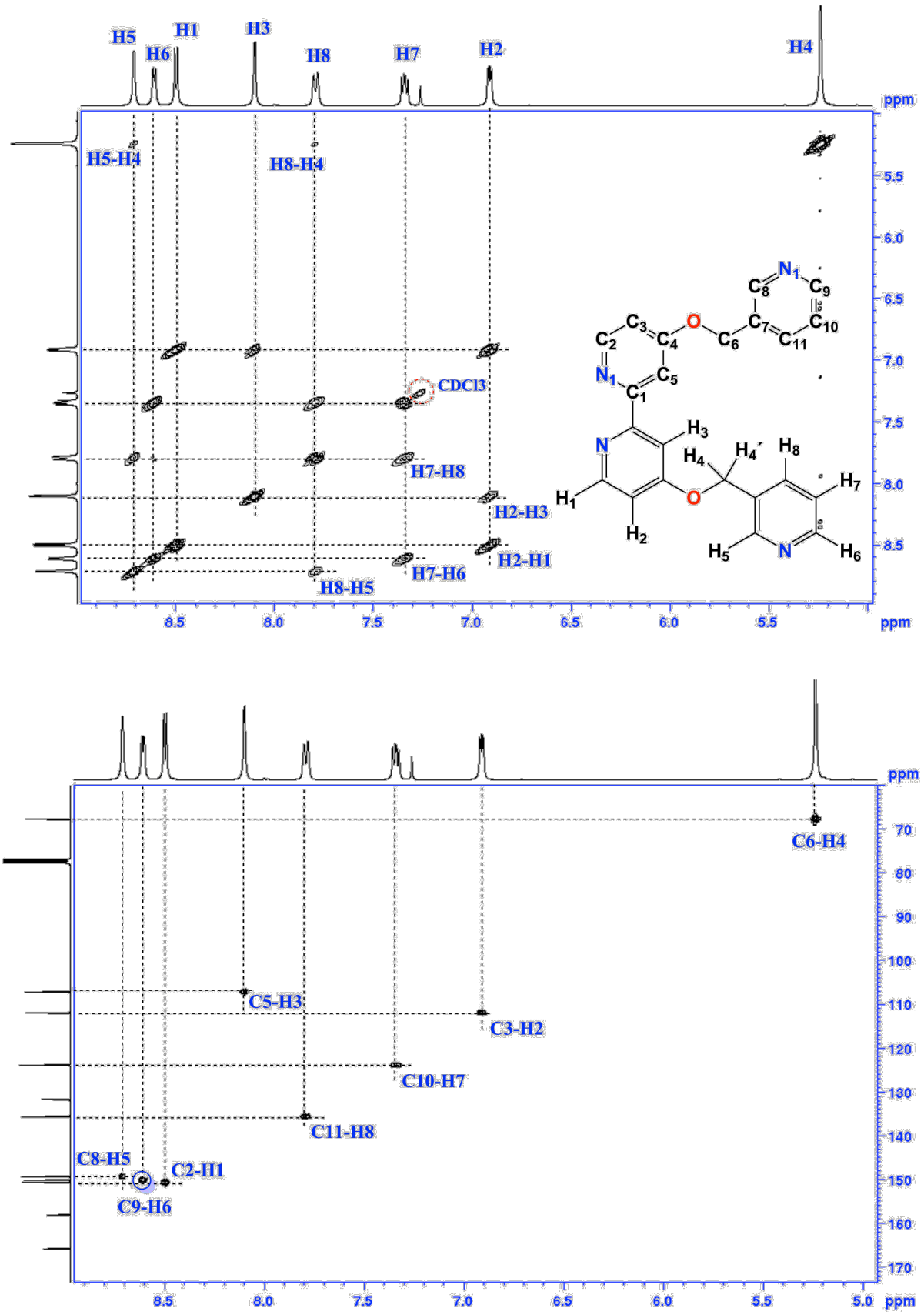

Fig. S16. 2-D NMR − COSY and HMQC for ligand **3** from $CDCl_3$.

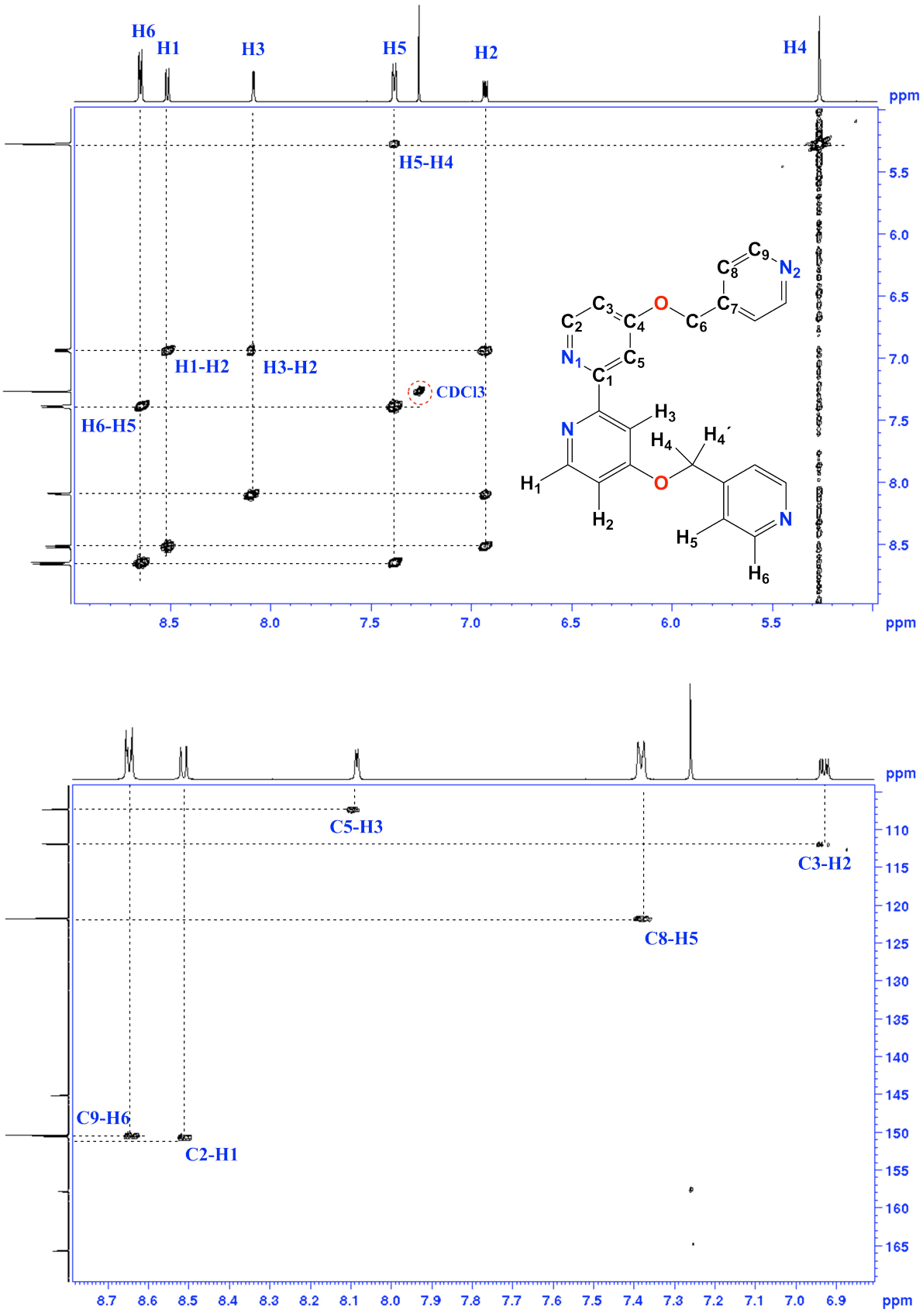

Fig. S17. 2-D NMR – COSY and HMQC for ligand **4** from $CDCl_3$.

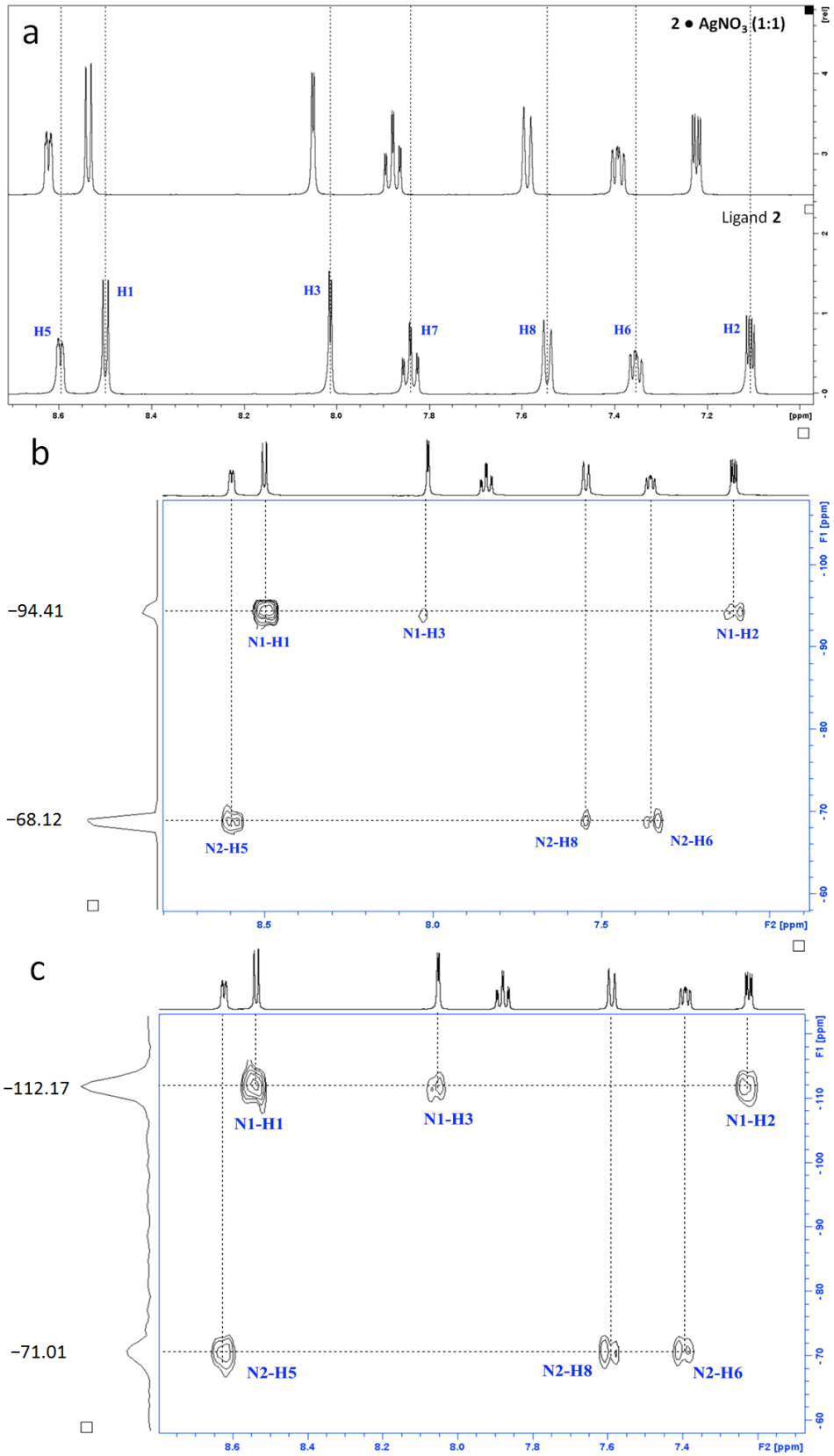

Fig. S18. The ^{1}H NMR spectra of ligand **2** and [**2•AgNO$_3$**] (a), ^{1}H-^{15}N 2D correlation spectrum of ligand **2** (b) and ^{1}H-^{15}N 2D correlation spectrum of ligand [**2•AgNO$_3$**] (c) in DMSO-d_6 at 70^{o}C (due to solubility issue at RT).

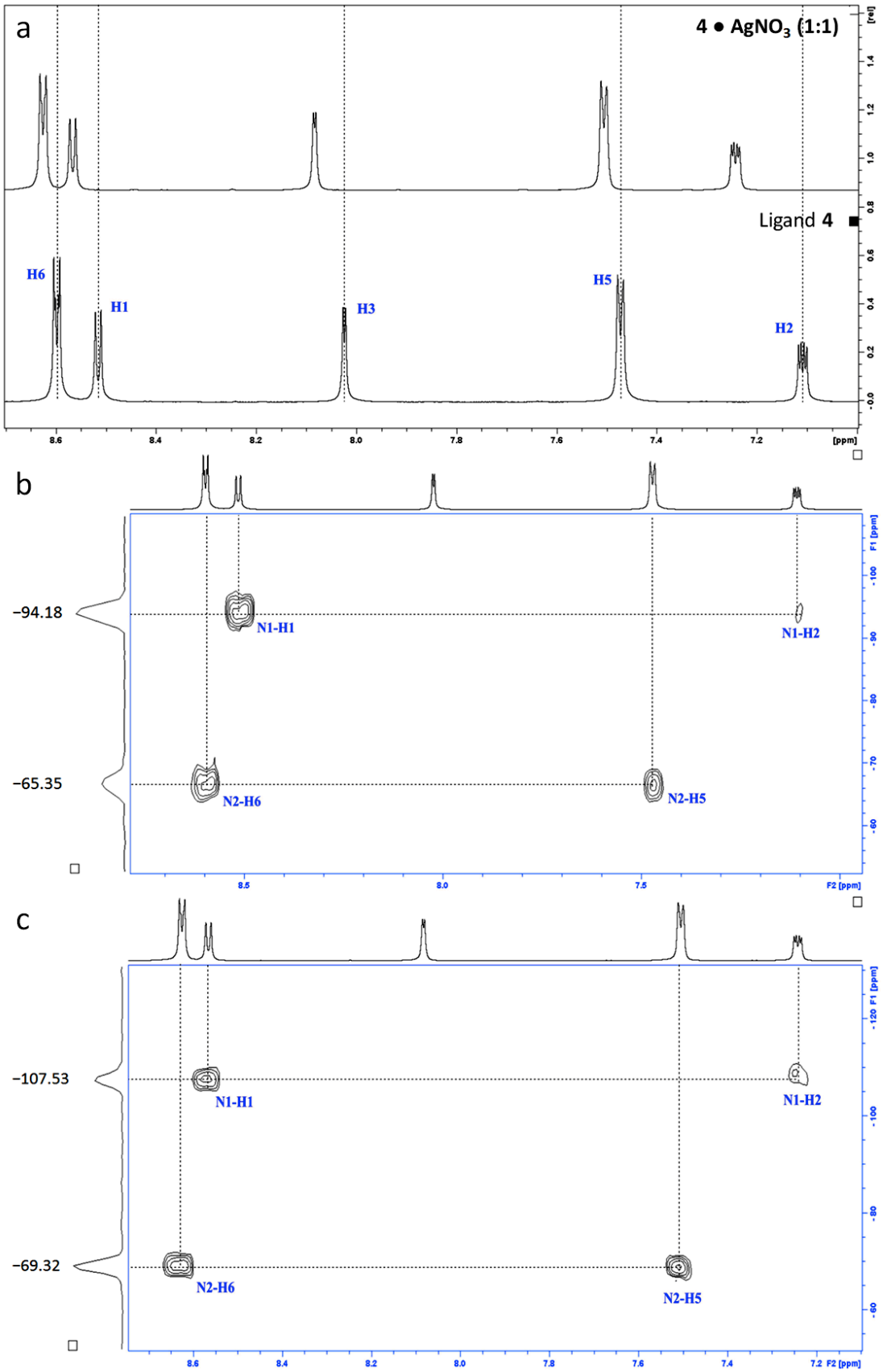

Fig. S19. The ^{1}H NMR spectra of ligand **4** and [**4•AgNO$_3$**] (a), ^{1}H-^{15}N 2D correlation spectrum of ligand **4** (b) and ^{1}H-^{15}N 2D correlation spectrum of ligand [**4•AgNO$_3$**] (c) in DMSO-d_6 at 70^{o}C (due to solubility issue at RT).

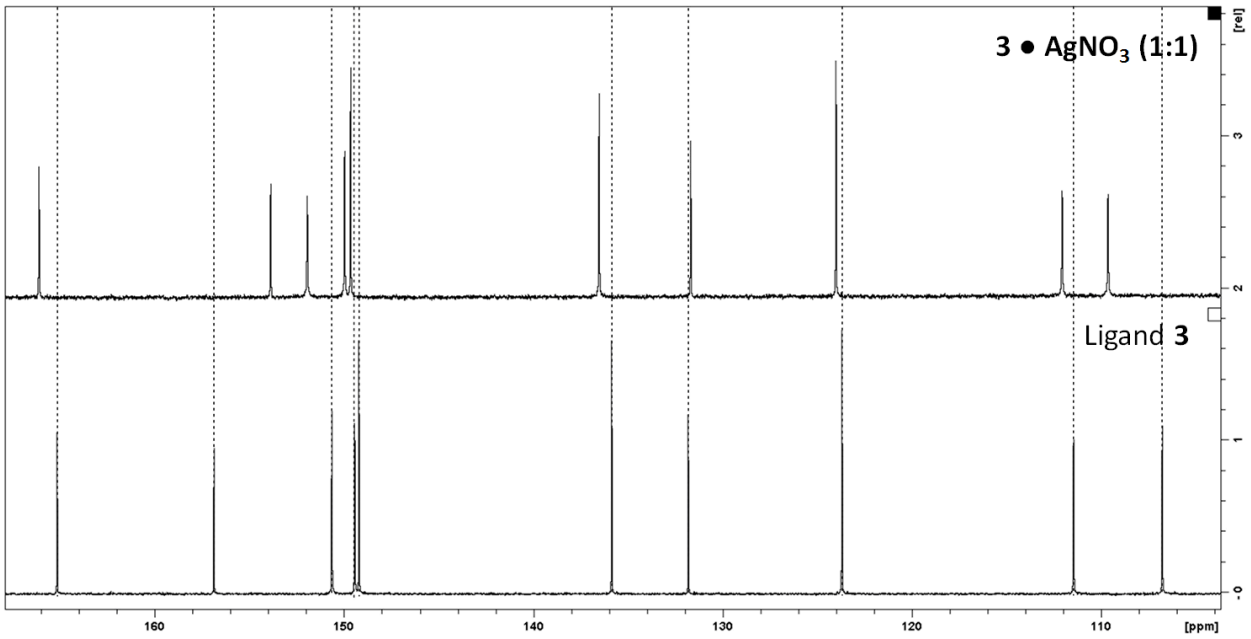

Fig. S20. ^{13}C NMR comparison of **3** and [**3●AgNO$_3$**] complex (1:1) in DMSO-d_6.

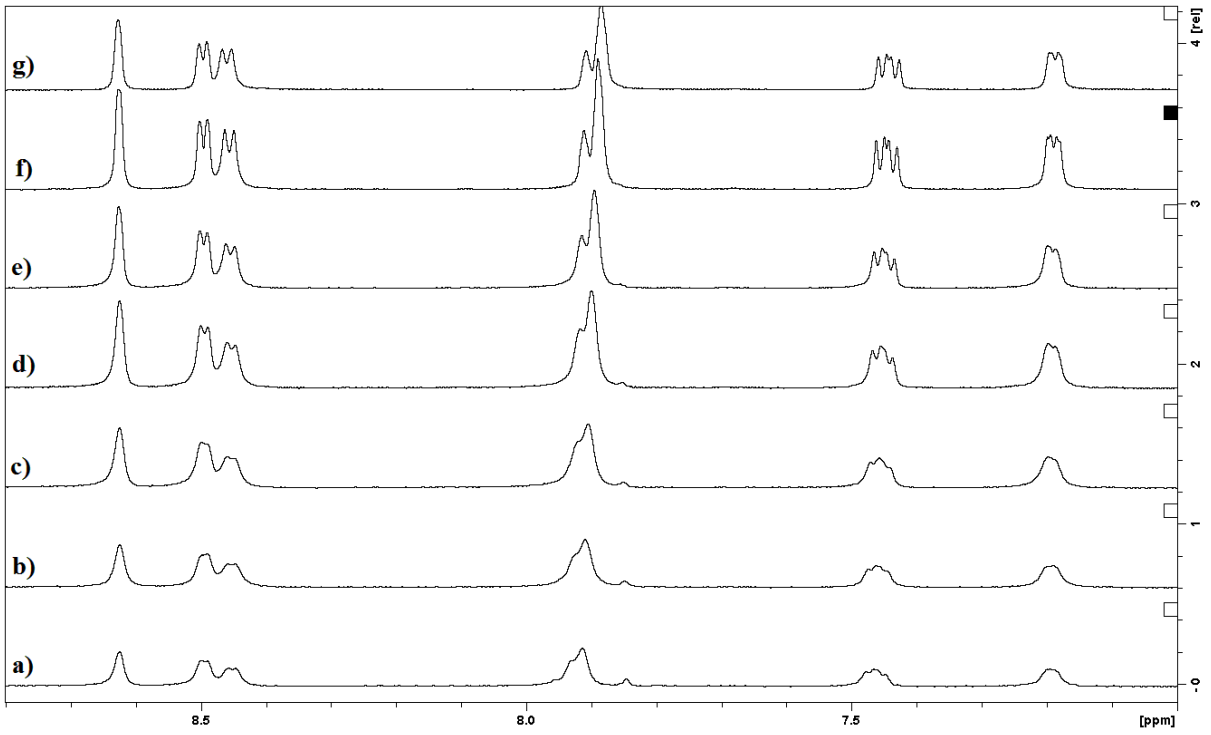

Fig. S21. Temperature dependent ^{1}H-NMR spectra of [**3●AgNO$_3$**] gel system from 6:4 of DMSO:H_2O (from 30 °C to 90°C, 10°C step increase).

7. Molecular modelling of the metallopolymers

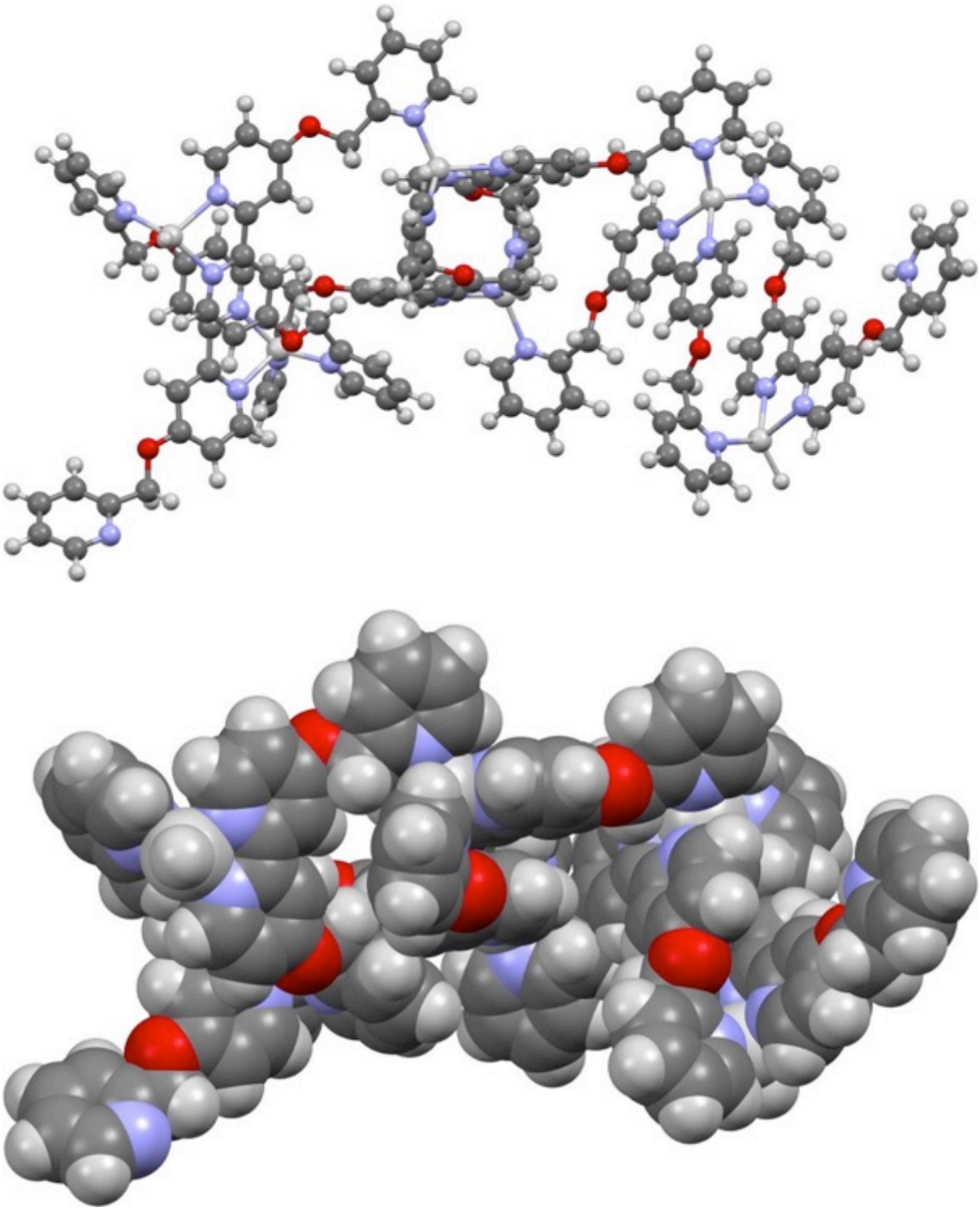

Fig. S22. The molecular model of the [**2**•**AgNO$_3$**] metallopolymer (MM force field, SPARTAN14[4])

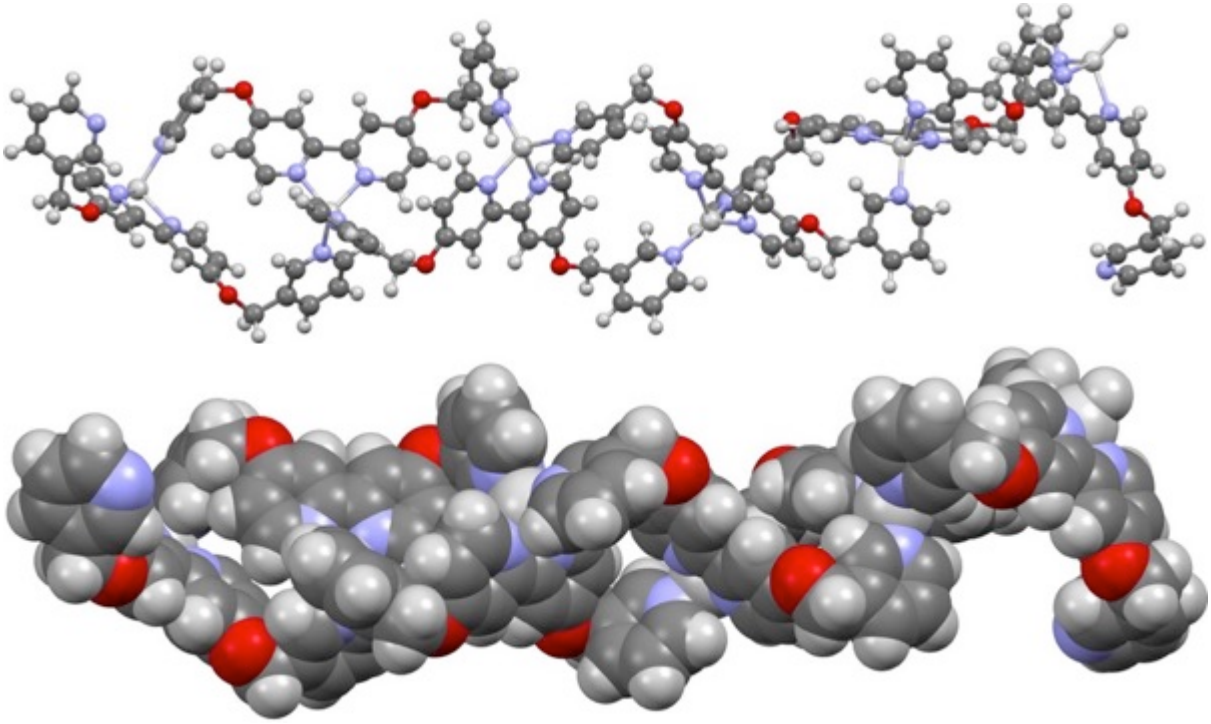

Fig. 23. The molecular model of the [**3**•**AgNO$_3$**] metallopolymer (MM force field, SPARTAN14[4])

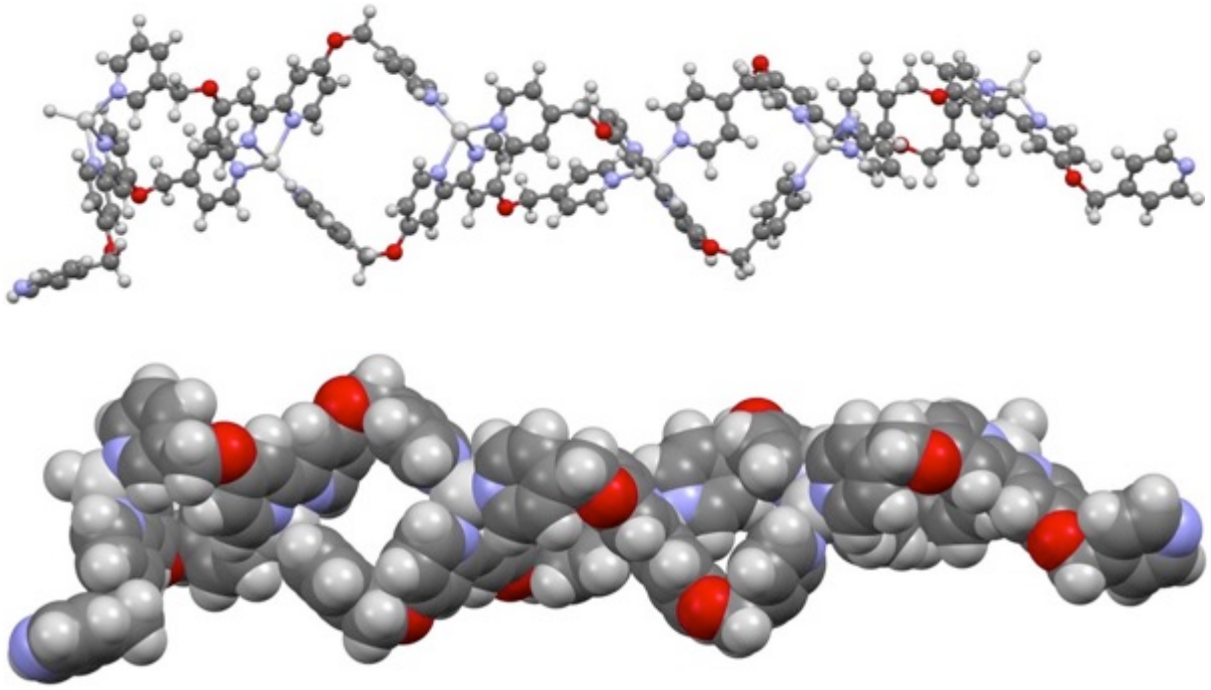

Fig. S24. The molecular model of the [**4**•**AgNO$_3$**] metallopolymer (MM force field, SPARTAN14[4]).

8. IR-Spectroscopy

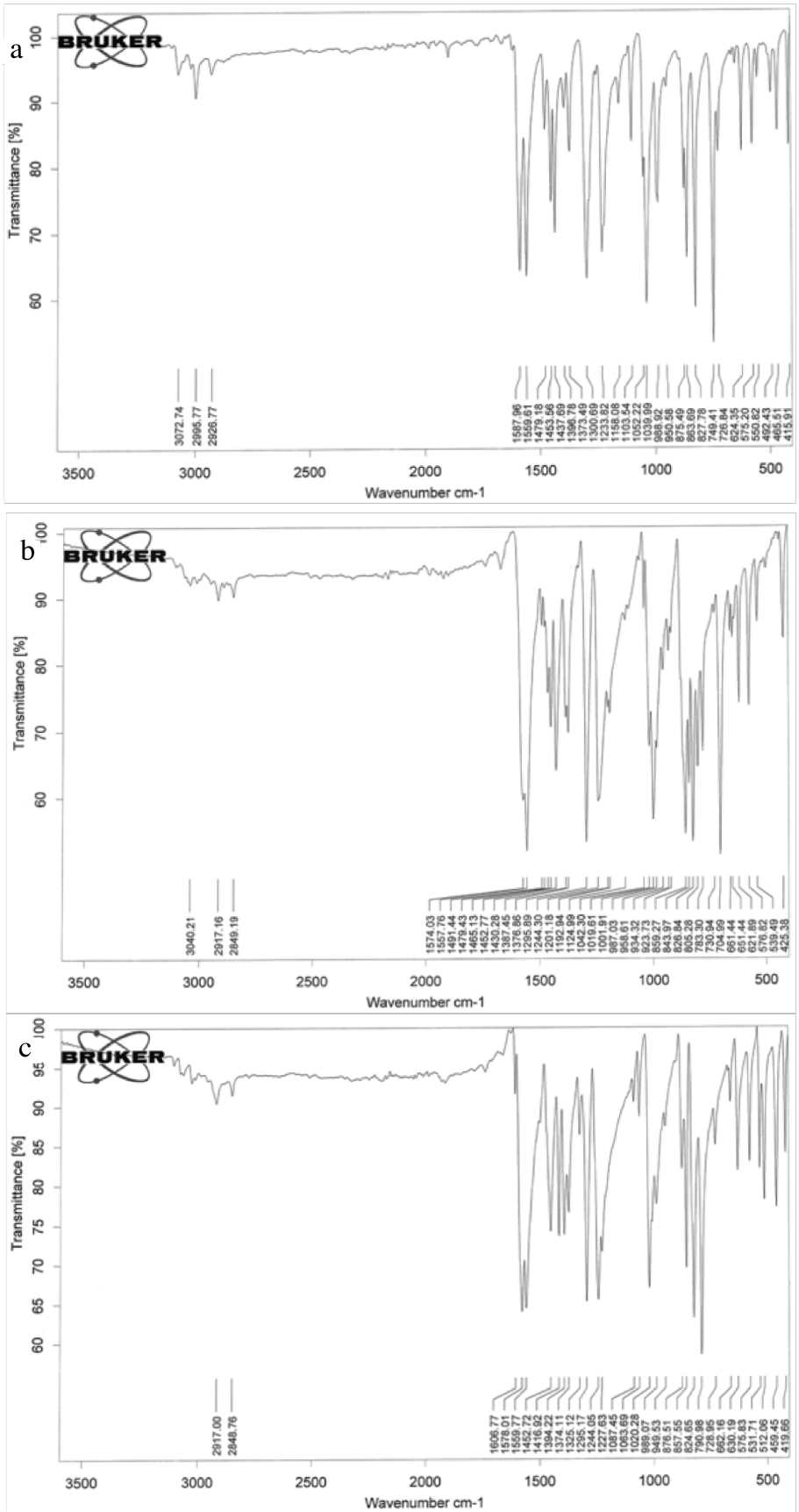

Fig. S25. FT-IR spectra of, a) ligand **2;** b) ligand **3** and d) ligand **4**.

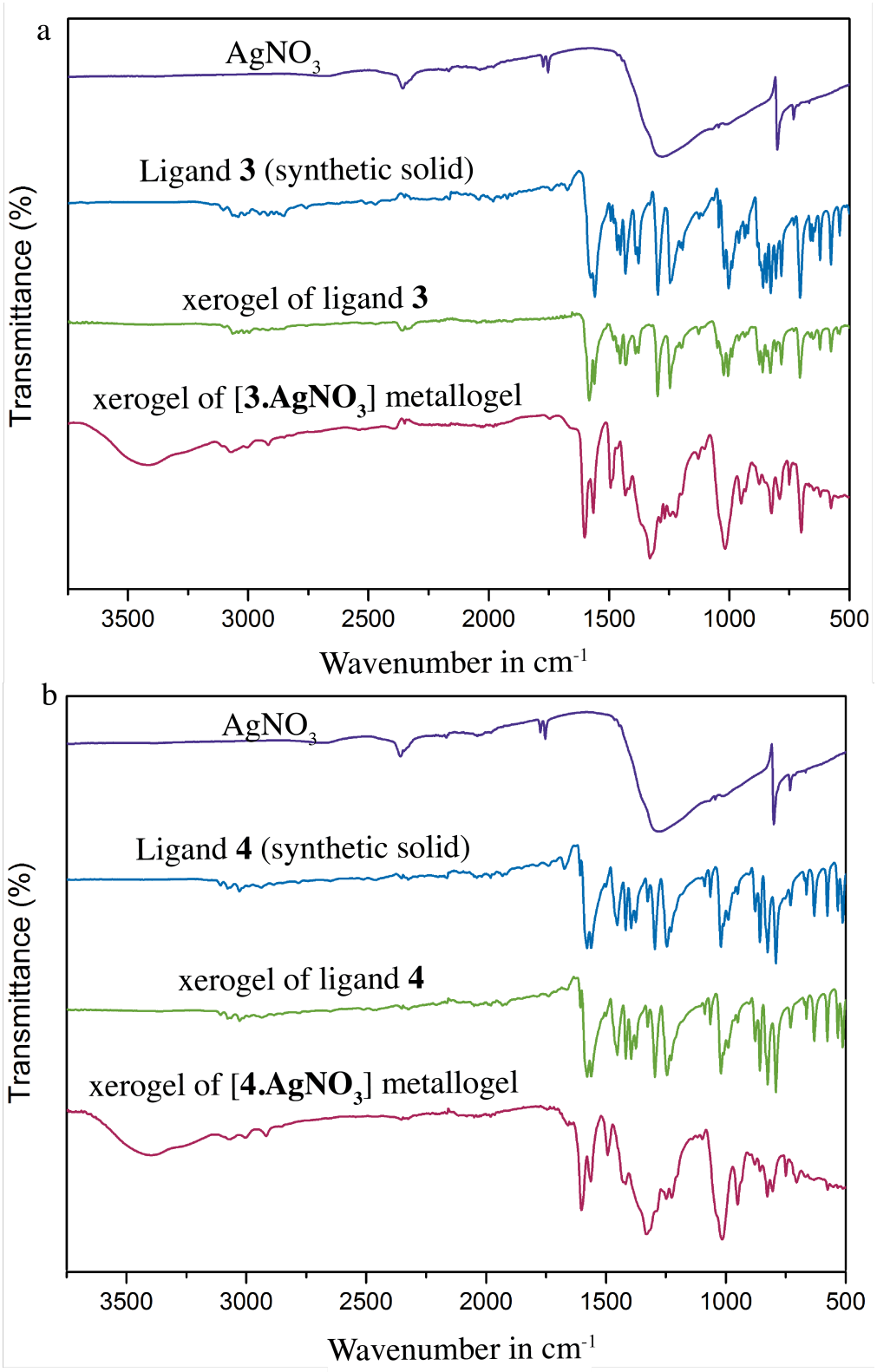

Fig. S26 Comparison of FT-IR spectra of ligands and metallogels derived from ligands **3** and **4**.

8. UV-Vis Spectroscopy

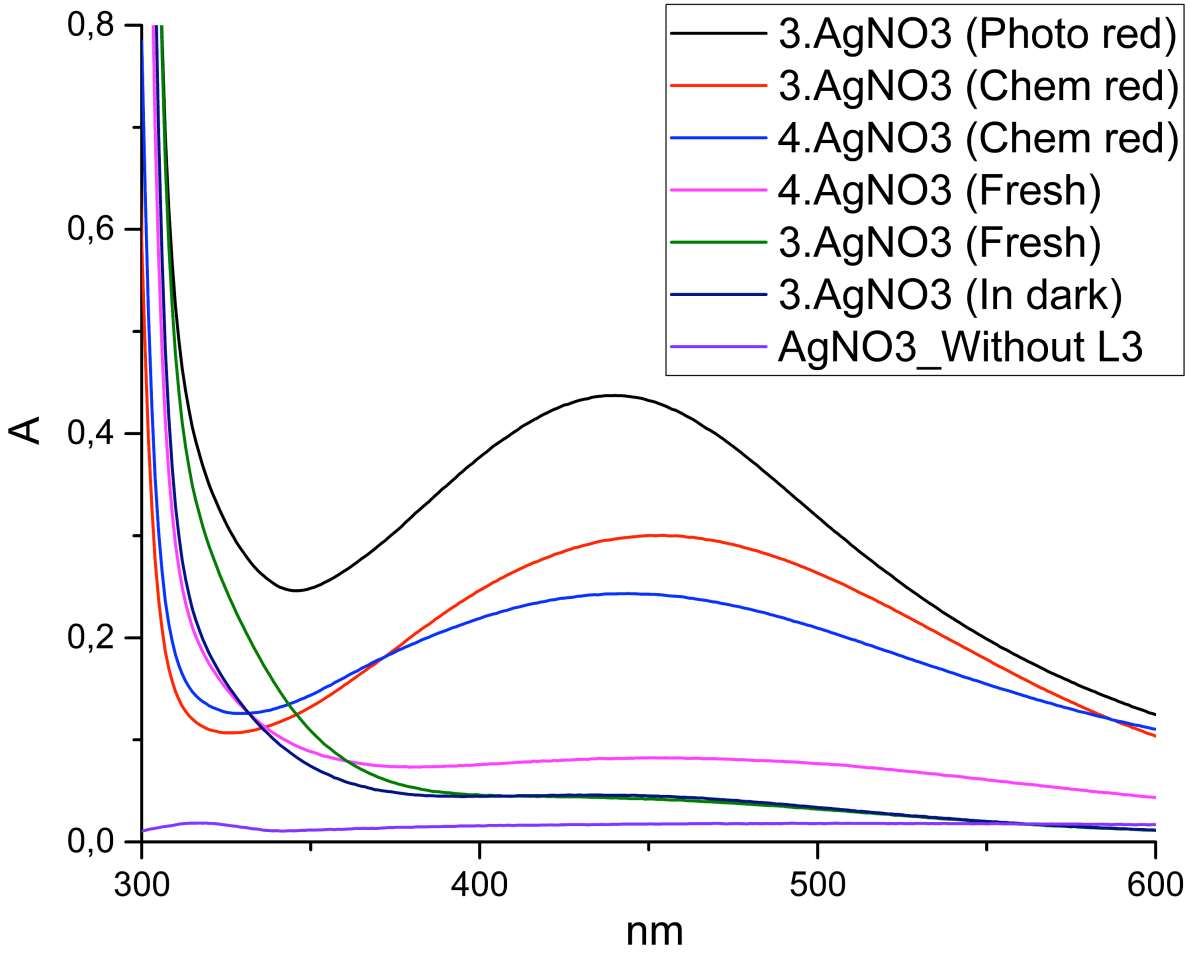

Fig. S27. UV-Vis Absorption spectra for [**3●AgNO$_3$**] (Fresh gel, Chemical reduction and Photochemical reduction), [**4●AgNO$_3$**] (Fresh gel and Chemical reduction) and control experiments with [**3●AgNO$_3$**] gel stroed in dark and only $AgNO_3$ in DMSO:H_2O.

Note. The same amount of gel samples were dissolved in DMSO and then measured.

9. Transmission electron microscopy (TEM)

The transmission electron microscopy (TEM) images were collected using FEI Tecnai G2 operated at 120 kV and JEM 3200FSC field emission microscope (JEOL) operated at 300 kV in bright field mode with Omega-type Zero-loss energy filter. The images were acquired with GATAN DIGITAL MICROGRAPH software while the specimen temperature was maintained at -187^{o}C. The TEM samples were prepared by placing 3-5 µL of the pre-made gel on to a 300 mesh copper grid with holey carbon support film. The samples were dried under ambient condition prior to imaging.

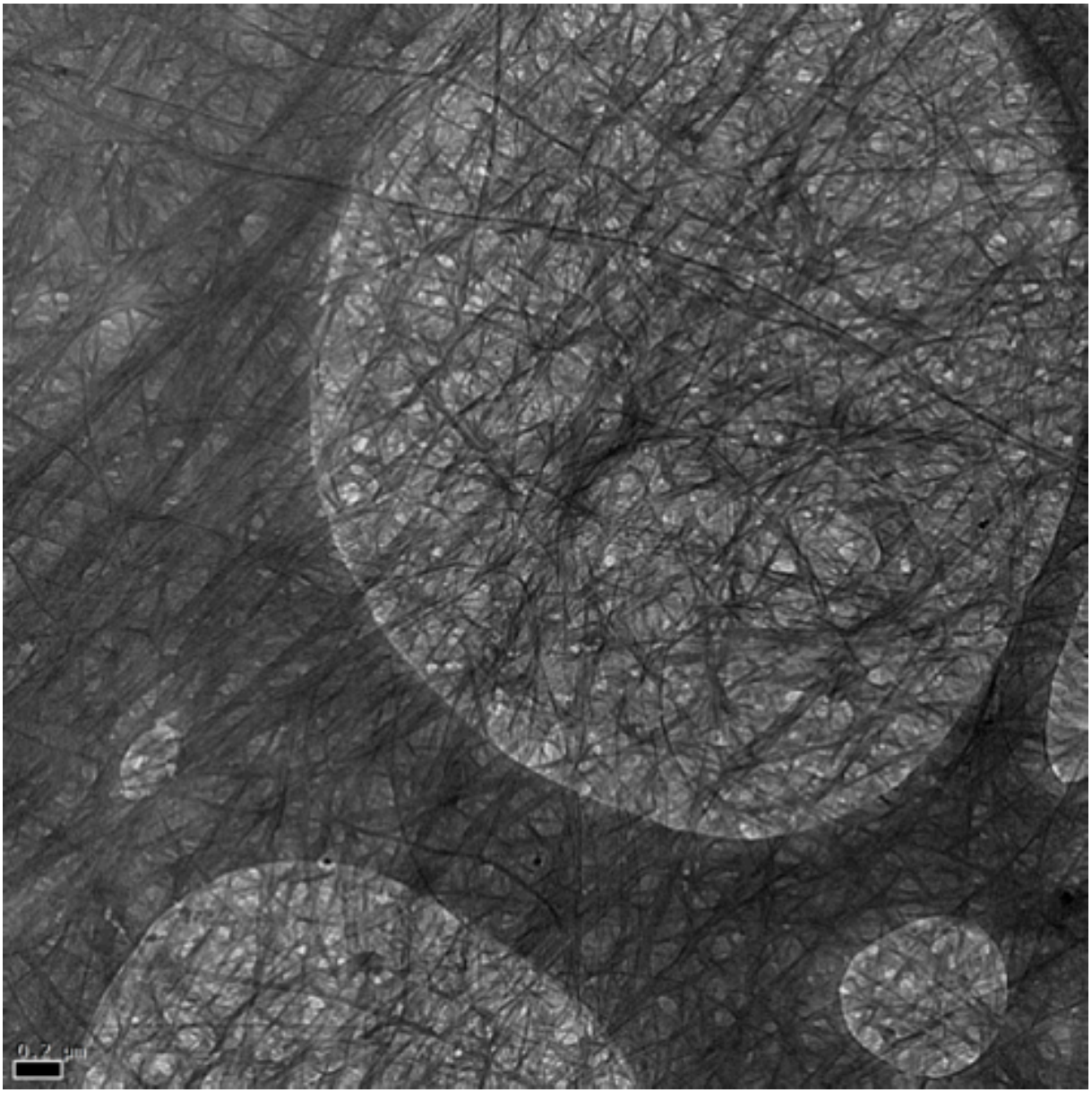

Fig. S28. TEM micrographs of freshly prepared DMSO/H_2O gel of [**3●AgNO$_3$**].

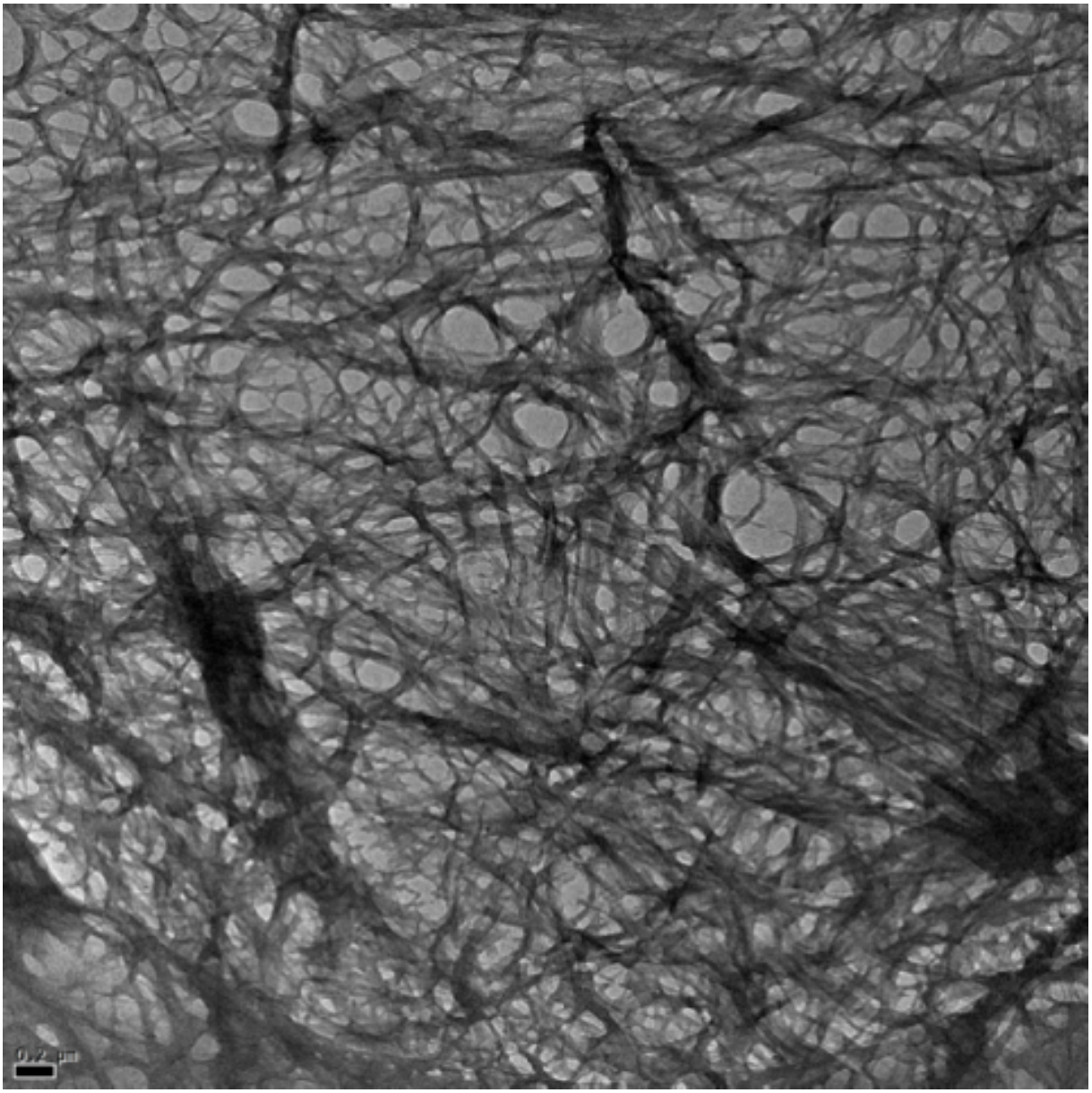

Fig. S29. TEM micrographs of freshly prepared DMSO/H_2O gel of [**4●AgNO$_3$**].

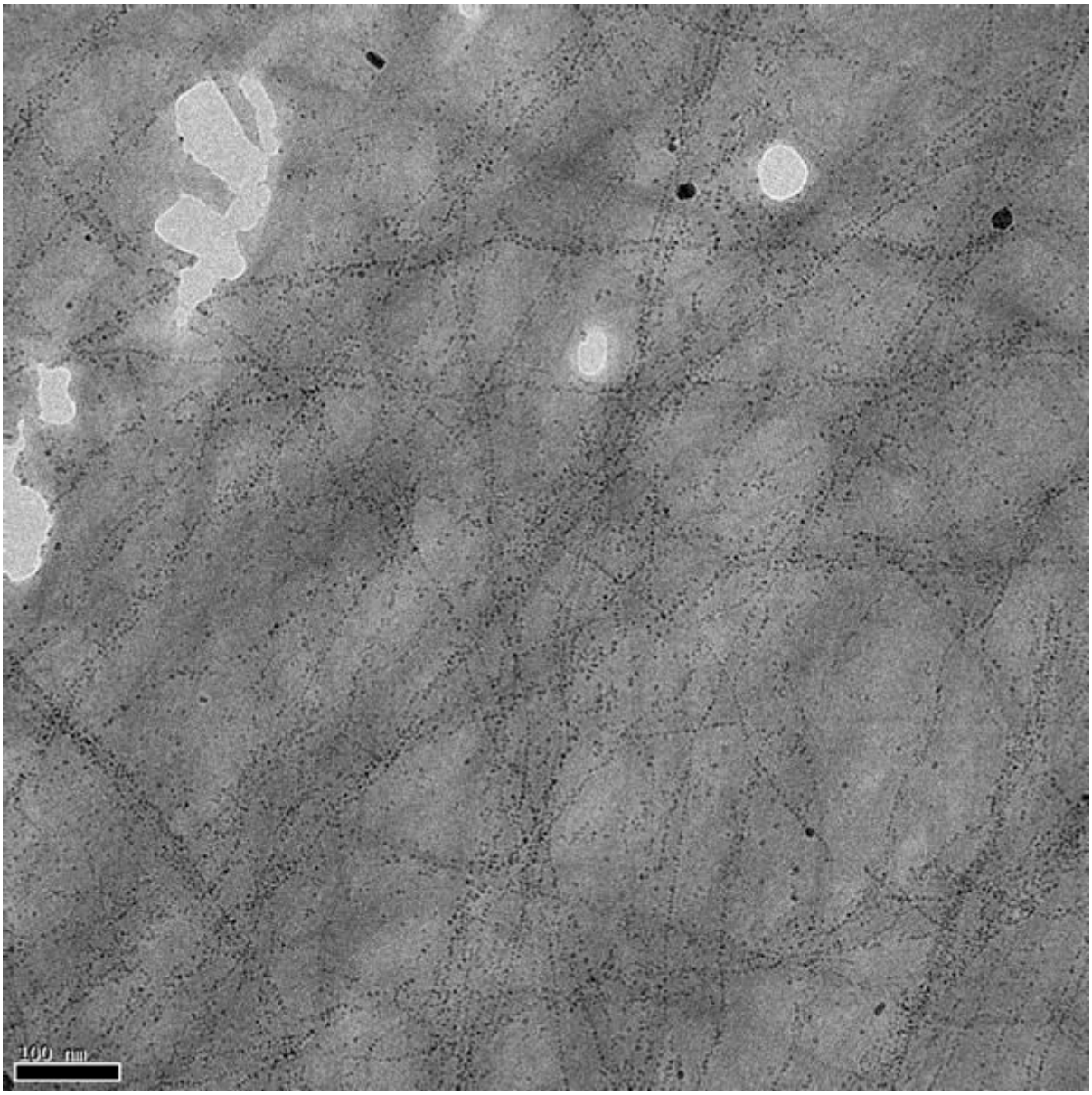

Fig. S30. TEM micrographs of daylight reduced DMSO/H_2O gel of [**3●AgNO$_3$**].

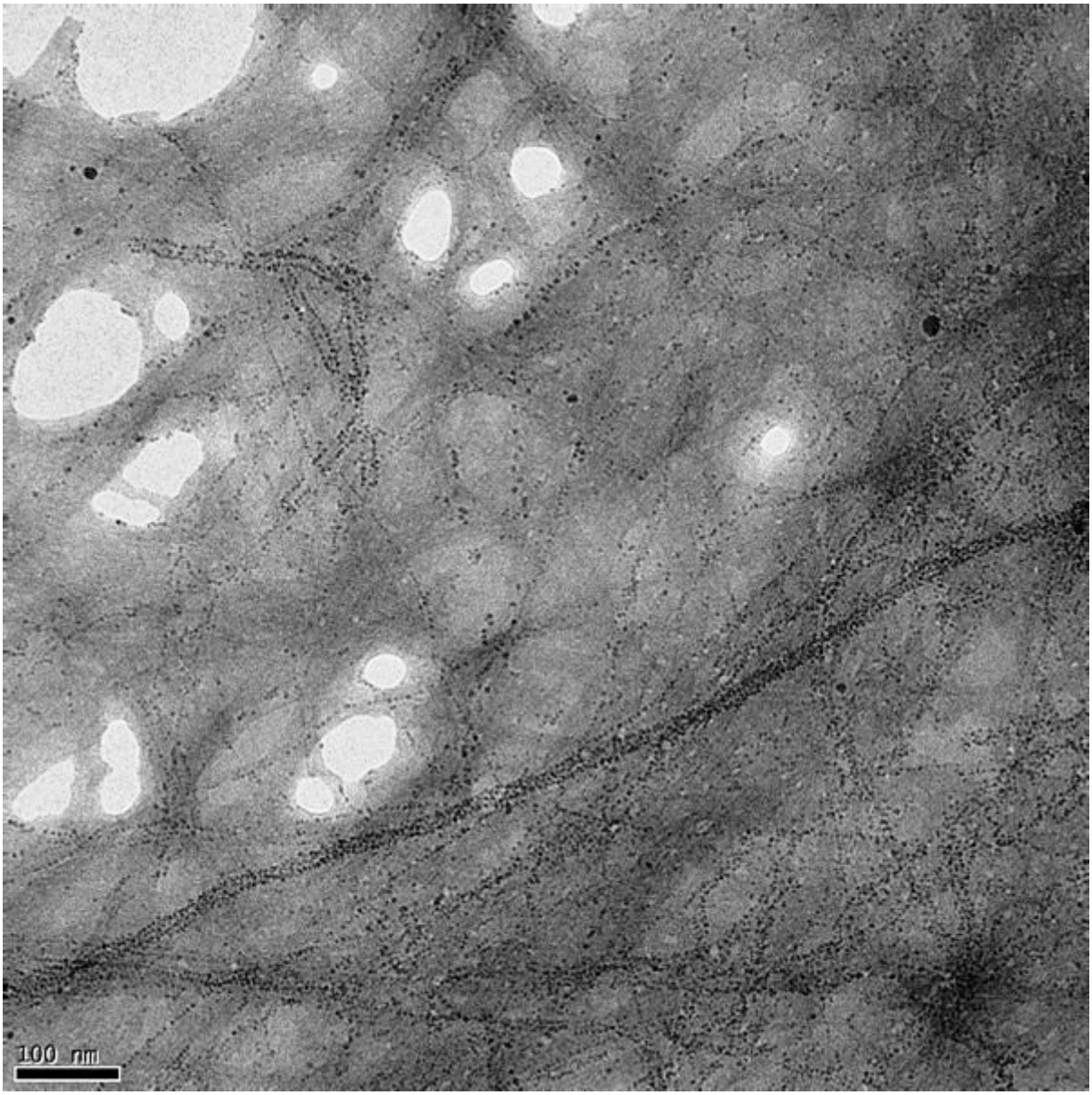

Fig. S31. TEM micrographs of daylight reduced DMSO/H_2O gel of [**3●AgNO$_3$**].

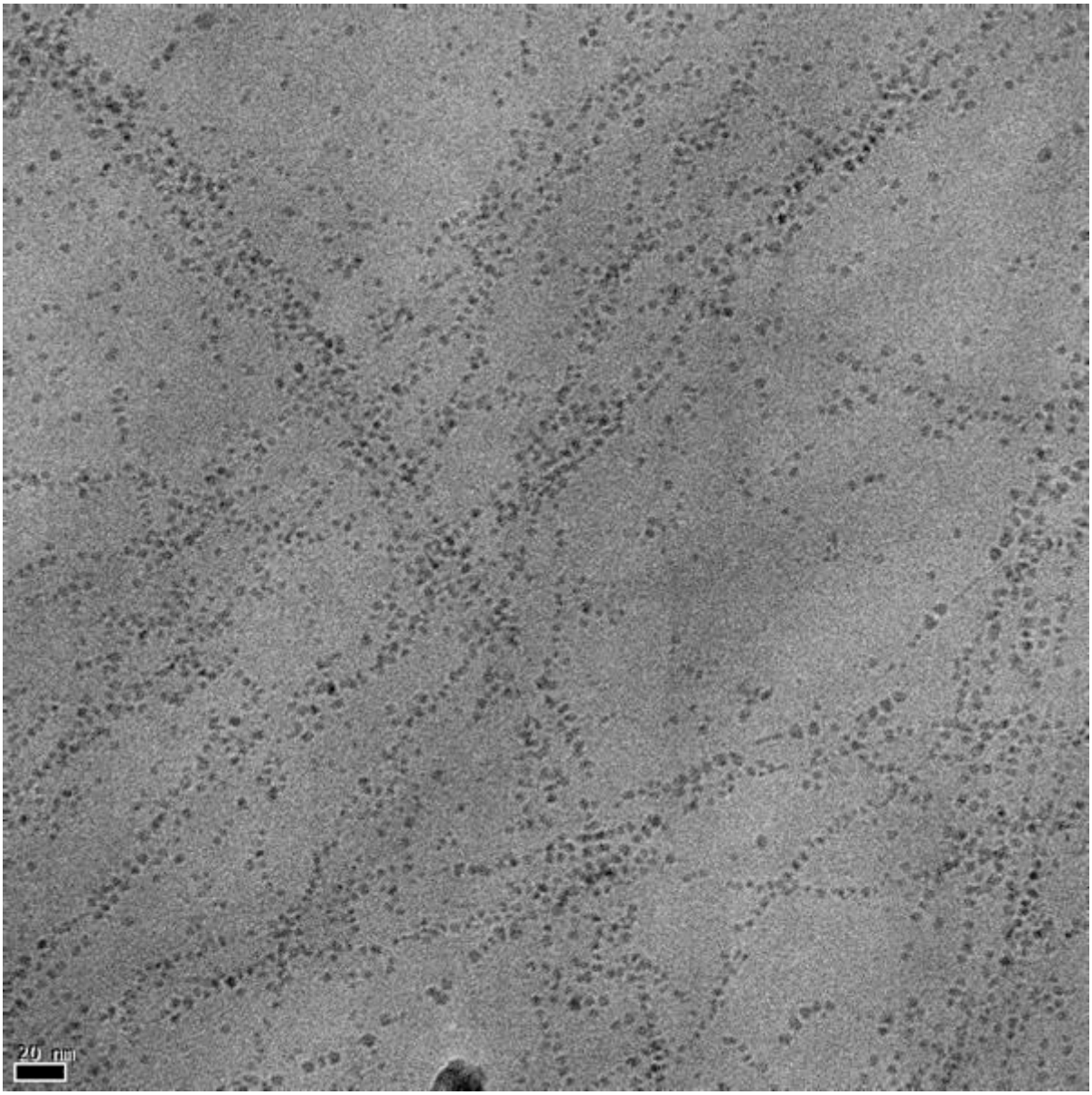

Fig. S32. TEM micrographs of daylight reduced DMSO/H_2O gel of [**3●AgNO$_3$**].

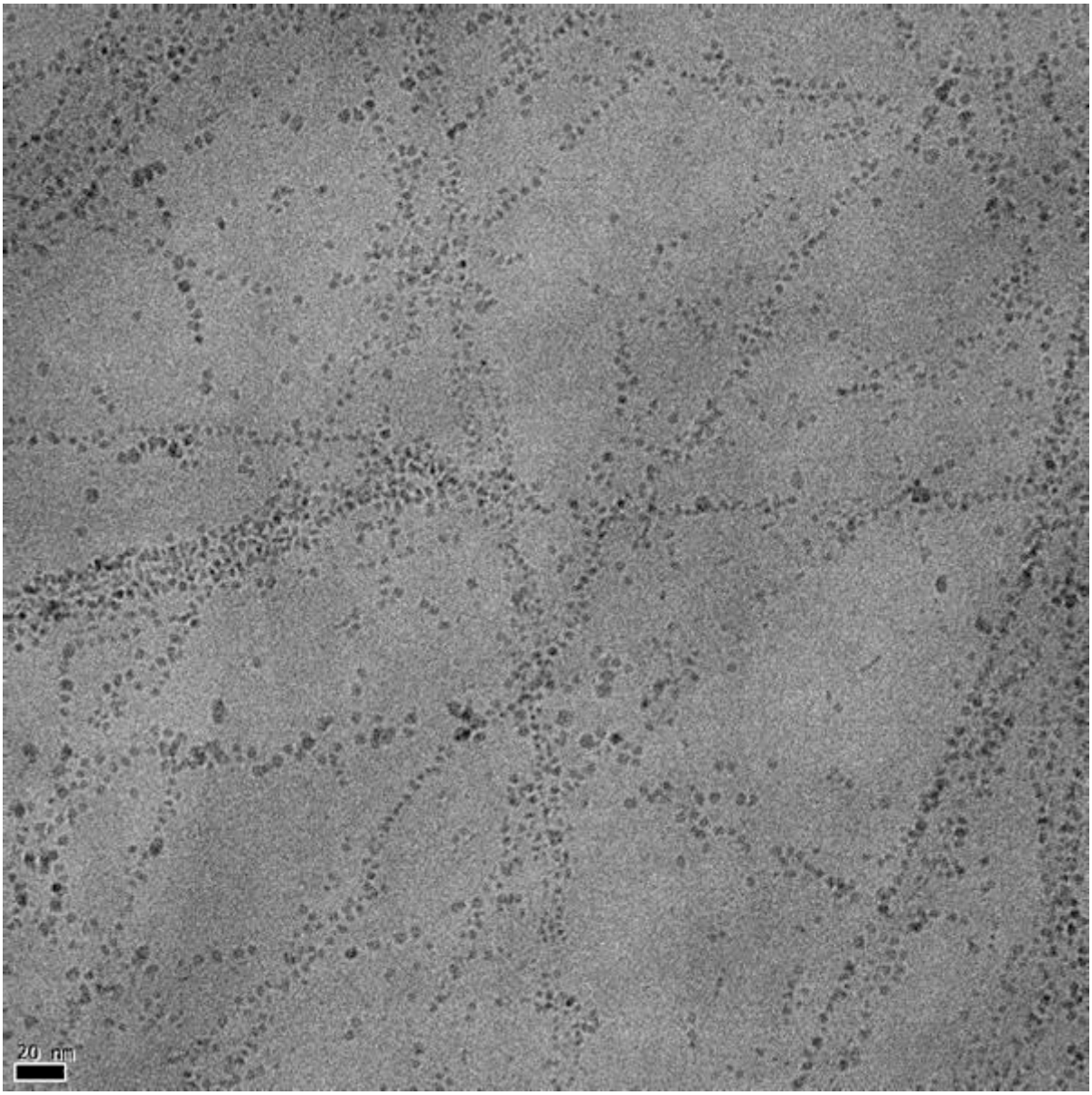

Fig. S33. TEM micrographs of daylight reduced DMSO/H_2O gel of [**3●AgNO$_3$**].

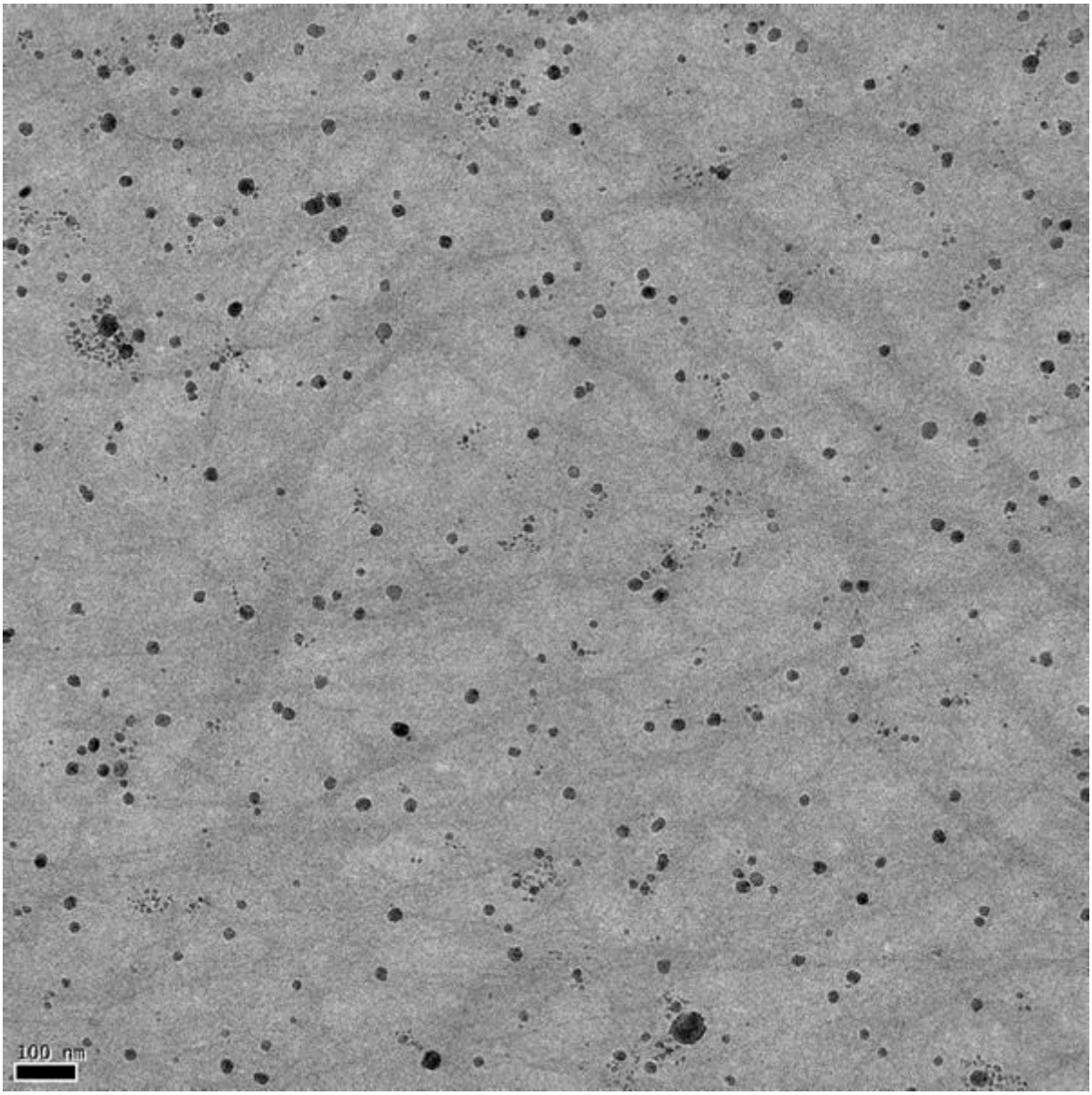

Fig. S34. TEM micrographs of $NaBH_4$ reduced DMSO/H_2O gel of [**3●AgNO$_3$**].

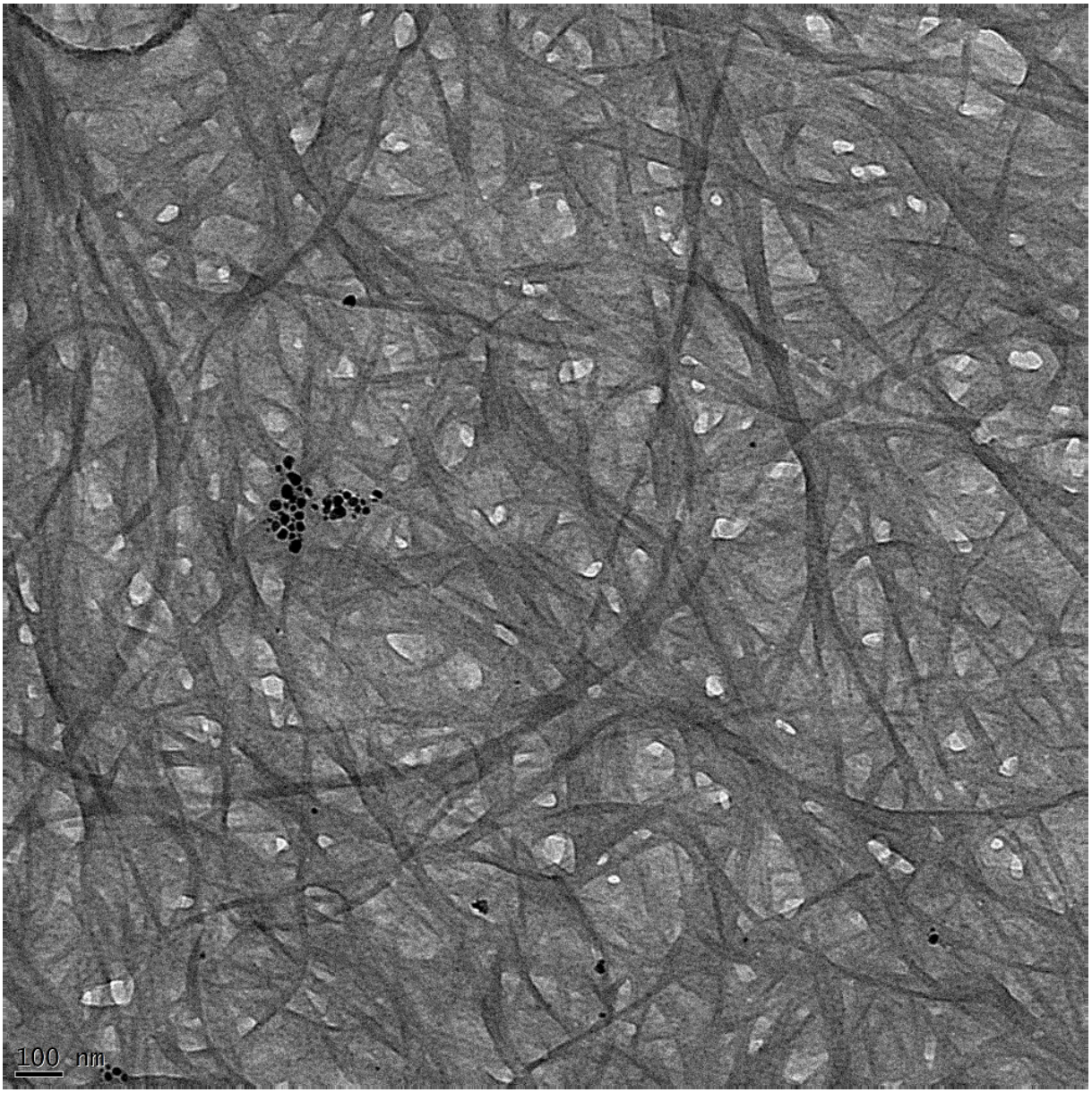

Fig. S35. TEM micrographs of freshly prepared DMF/H_2O gel of [**3●AgNO$_3$**].

References

1 Agilent, CrysAlisPro, *Agilent Technologies inc.* 2013, Yarnton, Oxfordshire, England.
2 L. Palatinus and G. Chapuis, *J. Appl. Cryst.,* 2017, **40**, 786.
3 G. M. Sheldrick, *Acta Cryst.,* 2008, **A64**, 112.
4 Spartan'14, Wavefunction, Inc., Irvine, USA.